

# NUCLEAR SPIN CONVERSION IN POLYATOMIC MOLECULES

*P.L. Chapovsky*

Institute of Automation and Electrometry, Russian Academy of Sciences,  
630090 Novosibirsk, Russia;  
E-mail: chapovsky@iae.nsk.su

*L.J.F. Hermans*

Huygens Laboratory, Leiden University, P.O. Box 9504, 2300 RA Leiden, The Netherlands;  
E-mail: hermans@molphys.leidenuniv.nl

KEYWORDS: spin-isomer enrichment, ortho-para conversion, hyperfine interactions, level-crossing, Zeno effect

**ABSTRACT:** Except for ortho- and para-H<sub>2</sub>, very little is known about nuclear spin isomers (or spin modifications) of molecules. The main reason is the lack of practical enrichment techniques. Recently a few enrichment methods were developed, which opened up new possibilities in the field. These methods are briefly reviewed. Substantial progress in the field has been made by the introduction of Light-Induced Drift as a gas-phase separation tool. This is illustrated by extensive data on CH<sub>3</sub>F, which reveal that the gas-phase ortho-para conversion is governed by intramolecular mixing of the nuclear spin states. The role of “direct” ortho-para transitions is shown to be small. Various aspects of the conversion were investigated in detail: pressure and collision partner dependence, isotope effect, temperature dependence. The most decisive information on the spin conversion mechanism is derived from the observation of level-crossing resonances in an electric field and the Quantum Zeno effect induced by collisions.

## CONTENTS

INTRODUCTION . . . . .	2
<i>Hydrogen spin isomers</i> . . . . .	2

<i>Other molecules</i> . . . . .	3
THEORY . . . . .	6
<i>Quantum relaxation</i> . . . . .	6
<i>Ortho-para state mixing in CH<sub>3</sub>F</i> . . . . .	10
<i>CH<sub>3</sub>F level structure and theoretical conversion rates</i> . . . . .	12
EXPERIMENTAL METHOD . . . . .	14
<i>Spin isomer separation by LID</i> . . . . .	14
<i>Relaxation time measurement</i> . . . . .	16
EXPERIMENTAL RESULTS . . . . .	17
<i>Dependence on pressure and collision partner</i> . . . . .	18
<i>Isotope effect</i> . . . . .	19
<i>Temperature dependence</i> . . . . .	19
<i>Level-crossing resonances</i> . . . . .	20
<i>Quantum Zeno effect induced by collisions</i> . . . . .	21
DIRECT ORTHO-PARA TRANSITIONS IN CH <sub>3</sub> F . . . . .	23
<i>Direct conversion on surfaces</i> . . . . .	23
<i>Direct conversion by collisions</i> . . . . .	24
CONCLUSION . . . . .	25
ACKNOWLEDGMENTS . . . . .	27

## 1 INTRODUCTION

### 1.1 Hydrogen spin isomers

At the beginning of the century physicists were puzzled by two seemingly unrelated phenomena: the anomalous specific heat of hydrogen discovered by Eucken in 1912 [1] and the line intensity alternation in molecular spectra discovered by Mecke in 1925 [2]. The solution of these two problems was a landmark in the foundation of quantum mechanics. As was pointed out by Farkas, “it was a real triumph for theory when in 1929 Bonhoeffer and Harteck [3] succeeded in bringing forward experimental evidence for the existence of the two different modifications of hydrogen” [4].

Three quarters of a century later, the explanation of these problems looks

almost trivial. There are two nuclear spin isomers of  $\text{H}_2$  which differ by total spin ( $I$ ) of the two hydrogen nuclei:  $I = 1$  for ortho hydrogen and  $I = 0$  for para hydrogen. The symmetry of the molecular wave function upon interchange of the two protons allows only odd values of rotational angular momentum ( $J$ ) for ortho and only even values of  $J$  for para. The spin isomers of  $\text{H}_2$  are extremely stable, having a conversion time on the order of 1 year at room temperature and 1 atm for pure hydrogen [4].

It is useful to recall the principle of the hydrogen spin isomer separation. A unique property of hydrogen molecules is their anomalously big rotational level spacing. The energy gap between the  $J=0$  and  $J=1$  states (first para and ortho states of hydrogen, respectively) is  $\simeq 170$  K. This energy gap is much larger than the boiling point of liquid hydrogen (20.4 K). The standard method of hydrogen isomer separation consists of cooling down the gas to 20.4 K in the presence of a catalyst (like activated charcoal or  $\text{Fe}(\text{OH})_3$ ) which speeds up the equilibration. After equilibrium is reached, 99.8% of the hydrogen molecules are in the lowest rotational state  $J=0$  which is the para state. After warming up the gas, one has pure para hydrogen at ambient temperatures because of extremely slow ortho-para conversion.

The discovery of hydrogen spin isomers triggered extensive investigations into their physical, chemical and even biological properties. Contrary to the intuitive feeling that nuclear spins are “deeply hidden” inside the molecule and cannot be important in practice, they play a decisive role in some practical problems. The most famous example is the storage of liquid hydrogen, e.g., as a rocket fuel, where considerable boil-off is caused by the energy released from ortho-para conversion. Research on hydrogen spin isomers, over nearly 70 years, has been reviewed in a few monographs [4, 5, 6, 7, 8] and is not considered in this paper.

## 1.2 Other molecules

The study of molecular spin isomers gave the first experimental background for the concept of nuclear spin (see, e.g., [9]), finally establishing the general relation between spin and statistics of identical particles. For molecular physics this theorem has as a consequence that molecules having identical nuclei in symmetrical positions (e.g.,  $\text{H}_2$ ,  $\text{NH}_3$ ,  $\text{CH}_4$ ,  $\text{N}_2$ , etc.) occur in nature only in the form

of nuclear spin isomers for which selection rules prescribe particular rotational quantum numbers to particular spin states.

Nuclear spin isomers of molecules other than hydrogen formed a long standing puzzle. Even 50 years after the discovery of hydrogen spin isomers one could safely state that “no one has ever produced gaseous samples of any molecules other than  $\text{H}_2$  or  $\text{D}_2$  in which the ratio of the concentrations of the different nuclear spin symmetry species is different from the high temperature equilibrium value” [10]. Thus, on one hand, quantum mechanics predicted the existence of stable spin isomers (see, for example, [11], p. 426), and on the other hand, almost nothing was known about their stability and their properties, for lack of practical separation methods. The simple technique of hydrogen isomer separation obviously fails in the case of heavy molecules, which have much smaller rotational level splitting and a much higher boiling point. Consequently, at temperatures sufficiently low for isomer enrichment the gas becomes solid. Thus the separation of spin isomers of heavy molecules requires a special technique. This is a non-trivial problem because spin isomers have identical masses and quite similar physical and chemical properties. Nevertheless, separation methods are under development now. In this Section we briefly review these methods.

- Low-temperature solids. Small molecules embedded in special matrices partially retain their spin isomer features. This allows one to produce in solids at low temperature significant enrichment of spin isomers in comparison with their abundance at room temperature. One may hope that the enrichment will be retained after fast evaporation of these molecules into the gas phase. In paper [12] an attempt was made to separate spin isomers of methane using rapid heating of a solid held at low temperature. In a subsequent paper [13] (see also [14]), these authors attributed the negative result of [12] to fast conversion due to the degeneracy of methane states having different spin symmetry. Yet this issue deserves further investigation because fast (although in a different time range) cooling of methane in a molecular jet is not accompanied by spin conversion [15, 16, 17].

- Selective photolysis. Due to the difference in allowed rotational quantum numbers, different spin isomers are spectroscopically distinguishable. (In fact, this is the essence of the famous line intensity alternation effect). In the enrichment method proposed in [13] narrow band laser radiation destroys one of the

spin isomers from an equilibrium mixture by photolysis. This method was first applied to the enrichment of  $I_2$  spin isomers [18]. It is not certain yet if  $I_2$  can be enriched by selective photolysis because the results [18] could not be reproduced in [19].

Selective photolysis was used for enrichment of spin isomers of formaldehyde ( $CH_2O$ ) molecules in [20]. The authors obtained enriched hydrogen (one of the photolysis products), but enrichment of  $CH_2O$  was not achieved. The conclusion was that the spin conversion is too fast in comparison with the duration of the photolysis [20]. Later, with an improved setup, enrichment of  $CH_2O$  spin isomers by selective photolysis was nevertheless demonstrated [21]. Those authors measured the life time of the formaldehyde spin isomers to be 200 sec. As a possible mechanism of conversion the authors [21] proposed the mixing of states model [13].

- Exchange reactions. Another approach to the separation of spin isomers of heavy molecules is based on the use of chemical exchange reactions with spin-polarized atoms. This technique proved feasible for the enrichment of nuclear spin isomers of diatomic molecules in [22, 23] where enrichment of  $Na_2$  and  $Li_2$  was obtained.

- Selective adsorption/condensation. The difference in rotational quantum numbers for different spin isomers can cause a difference in their physical properties, e.g., in adsorption on surfaces. This can be used for separation. Thus spin isomers of water molecules were separated by selective condensation [24] and by selective adsorption on  $Al_2O_3$  surface [25]. This group measured the life time of water spin isomers to be  $4.4 \pm 0.2$  days. Presumably, the isomers convert on the container surface [25]. No model was proposed so far for the conversion of water.

- Chemical reactions. The dependence of chemical reactions on the nuclear spin state of the reacting molecules was predicted in [26]. This selectivity was employed in experiment [27] to obtain enriched samples of  $H_3^+$  molecules by chemical reactions involving enriched  $H_2$ .

- Light-induced drift. A breakthrough in the separation of spin isomers was achieved in Ref. [28] by using Light-Induced Drift (LID) [29].  $CH_3F$  isomer separation was analogous to the previously performed enrichment of the  $CH_3F$  isotope species (see [30] and references therein). The LID effect proved to be a convenient

tool since it enables one to separate spin isomers in the gas phase at well-defined gas composition, temperature and pressure. Although this technique can be applied to any molecular species in principle, the first experiments were performed on  $\text{CH}_3\text{F}$  for the following reasons. The two nuclear spin species, characterized by their total proton spin  $I=3/2$  or  $1/2$ , have well-distinguishable rovibrational absorption lines which are easily accessible by a  $\text{CO}_2$  laser. In addition,  $\text{CH}_3\text{F}$  is chemically inactive and has low adsorption onto the cell walls. These fortunate circumstances have promoted substantial progress in the field. The first measurement of the life time of nuclear spin isomers of polyatomic molecules was performed for  $^{12}\text{CH}_3\text{F}$  and gave 2 hours [31]. In subsequent measurements [32] nearly two orders of magnitude difference in the conversion rates of spin isomers of  $^{13}\text{CH}_3\text{F}$  and  $^{12}\text{CH}_3\text{F}$  molecules was observed.

At the time of these experiments the nuclear spin conversion of  $\text{CH}_3\text{F}$  molecules was considered to be a heterogeneous process. The situation changed when it was proven [33] that the  $\text{CH}_3\text{F}$  conversion is a gaseous process having an anomalously large isotope dependence  $(14 \pm 1) \times 10^{-3} \text{ s}^{-1}/\text{torr}$  for the  $^{13}\text{CH}_3\text{F}$  isomers and  $(0.31 \pm 0.03) \times 10^{-3} \text{ s}^{-1}/\text{torr}$  for the  $^{12}\text{CH}_3\text{F}$  isomers. Although these rates are extremely fast if compared to the  $\text{H}_2$  case, they are astonishingly slow if considered from a gas-kinetic point of view: the molecules retain their spin state even after suffering some  $10^9$  collisions which totally scramble the rotational state. The first feeling of a researcher in this situation is that the phenomenon is too complicated to expect a simple description based on first principles. Nevertheless, there is such simple model as will be shown below.

## 2 THEORY

### 2.1 Quantum relaxation

An explanation of the  $\text{CH}_3\text{F}$  spin conversion was suggested [33] in the framework of a model based on intramolecular mixing of ortho and para states of the molecule. This model was proposed in a theoretical paper by Curl et al [13] as a tentative mechanism of spin conversion in  $\text{H}_2\text{O}$ ,  $\text{CH}_2\text{O}$  and  $\text{CH}_4$ . The model [13] formed the basis of a new approach to the spin conversion in polyatomic molecules.

The essence of spin conversion induced by intramolecular mixing consists of the following. Let us divide the quantum states of a molecule into two subspaces, ortho and para, each having their own rotational energy levels. This is symbolized in Figure 1. Let us assume for simplicity that only one pair of ortho and para states ( $m$ - $n$ ) is mixed by an intramolecular perturbation. Suppose that at the beginning of the conversion process a test molecule is placed in the ortho subspace. Collisions of the test molecule with the surrounding particles cause fast migration inside the ortho subspace but cannot, by assumption, change its spin state directly. This running up and down along the ladder of ortho states continues until the molecule arrives in the state  $m$  which is mixed with the energetically close para state  $n$ . During the free flight after this collision, the para state  $n$  will be admixed by the internal perturbation to the ortho state  $m$ , which creates a coherent mixture of the  $m$  and  $n$  states. The next collision can destroy this coherent mixture of states by transferring the molecule to other para states. This will localize the molecule inside the para subspace, and conversion has taken place.

To summarize, the mechanism of spin conversion is based on intramolecular mixing of ortho and para states and collisional destruction of the coherence between the states. This type of relaxation deserves a special name and can be called “quantum relaxation” [35]. Processes of similar origin are well known in various parts of physics. First of all we can mention the relaxation of magnetic polarization in NMR [36]. Another example is the vibrational energy transfer enhanced by Coriolis perturbation (see [37] and references therein). The same mechanism is responsible for the singlet-triplet relaxation in spin-radical pairs [38]. Analogous mechanisms can be found also in elementary particle physics, e.g., neutral kaon decay [39].

Below we give a rigorous model of isomer conversion by quantum relaxation [33], hoping that the reader will enjoy seeing how a few steps of simple mathematics bring us to a general solution of a complicated problem. Suppose, that the molecular Hamiltonian is the sum of the two parts

$$\hat{H} = \hat{H}_0 + \hbar\hat{V}, \quad (1)$$

where  $\hat{H}_0$  is the main part of the Hamiltonian which has pure ortho and para states as the eigen states;  $\hat{V}$  is a small intramolecular perturbation which mixes

the ortho and para states.

The Liouville equation for the density matrix  $\rho$  of the molecule in the representation of the eigen states of the operator  $\hat{H}_0$  reads

$$(\partial/\partial t)\rho_{\alpha\alpha_1} = S_{\alpha\alpha_1} - i[\hat{V}, \rho]_{\alpha\alpha_1}, \quad (2)$$

where  $S_{\alpha\alpha_1}$  is the collision integral and  $\alpha$  and  $\alpha_1$  represent the complete sets of quantum states.

Using Eq.(2) one can obtain an equation which governs the change of molecular concentration in one particular nuclear spin state. This can be done by calculating the trace of Eq.(2) over all states of one spin isomer. For example, for the concentration of ortho molecules ( $\rho_o$ ) one has

$$(\partial/\partial t)\rho_o = 2Re \sum_{\alpha \in o, \alpha' \in p} i\rho_{\alpha\alpha'} V_{\alpha'\alpha}; \quad \rho_o \equiv \sum_{\alpha \in o} \rho_{\alpha\alpha}, \quad (3)$$

where  $\alpha$  runs over all ortho ( $o$ ) states and  $\alpha'$  runs over all para ( $p$ ) states. Henceforth, unprimed quantum numbers will refer to the ortho states, and the primed ones to the para states.

When deriving Eq.(3) we have assumed that collisions conserve the number of molecules in each spin state (no ‘‘direct’’ conversion). This can be expressed as

$$\sum_{\alpha \in o} S_{\alpha\alpha} = \sum_{\alpha' \in p} S_{\alpha'\alpha'} = 0. \quad (4)$$

This property means that the collisional cross-section of ortho-para transfer is equal to zero:  $\sigma(p|o)=0$ . The justification of the relations (4) for  $\text{CH}_3\text{F}$  molecules, both experimental and theoretical, can be found in [40, 41, 42].

To find the time dependence of  $\rho_o$  from Eq.(3) we need to know the off-diagonal matrix elements of  $\rho$ , which are a measure of the coherence between ortho and para states. From Eq.(2) we have

$$(\partial/\partial t)\rho_{\alpha\alpha'} = S_{\alpha\alpha'} - i[\hat{V}, \rho]_{\alpha\alpha'}. \quad (5)$$

In first order perturbation theory, on the right hand side of Eq.(5) one has to keep only the unperturbed values of the density matrix. Those are the diagonal matrix elements of  $\rho$ . This leads to the equation

$$(\partial/\partial t)\rho_{\alpha\alpha'} = S_{\alpha\alpha'} - iV_{\alpha\alpha'}(\rho_{\alpha'\alpha'} - \rho_{\alpha\alpha}). \quad (6)$$



Here we have assumed that perturbation  $\hat{V}$  has no diagonal matrix elements. Such definition of  $\hat{V}$  is always possible by proper separation (1) of the molecular Hamiltonian.

Further, we will model the off-diagonal elements of the collision integral solely by a decay process:  $S_{\alpha\alpha'} = -\Gamma_{\alpha\alpha'}\rho_{\alpha\alpha'}$ . The decoherence rate  $\Gamma_{\alpha\alpha'}$  is approximately equal to the average of the population decay rates in the states  $\alpha$  and  $\alpha'$ . Note that  $\Gamma_{\alpha\alpha'}$  is proportional to the gas pressure. Moreover, we assume all  $\Gamma_{\alpha\alpha'}$  to be equal:  $\Gamma_{\alpha\alpha'} \equiv \Gamma$ . Thus the off-diagonal terms of the collision integral will be modeled by the *Ansatz*

$$S_{\alpha\alpha'} = -\Gamma\rho_{\alpha\alpha'} . \quad (7)$$

The validity of this model will be tested below by comparison with experiment.

The intramolecular perturbation  $\hat{V}$  is time independent. Consequently, the time dependence of  $V_{\alpha\alpha'}$  is given by  $\exp(i\omega_{\alpha\alpha'}t)$  where  $\hbar\omega_{\alpha\alpha'}$  is the energy gap between the states  $\alpha$  and  $\alpha'$ . Using the assumptions made above, the steady-state solution of Eq.(6) reads

$$\rho_{\alpha\alpha'} = \frac{-iV_{\alpha\alpha'}}{\Gamma + i\omega_{\alpha\alpha'}}(\rho_{\alpha'\alpha'} - \rho_{\alpha\alpha}) . \quad (8)$$

Combining (3) and (8) one has

$$\frac{\partial\rho_o}{\partial t} = \sum_{\alpha \in o, \alpha' \in p} \frac{2\Gamma |V_{\alpha\alpha'}|^2}{\Gamma^2 + \omega_{\alpha\alpha'}^2}(\rho_{\alpha'\alpha'} - \rho_{\alpha\alpha}) . \quad (9)$$

The diagonal elements of the density matrix (which are populations of states) are determined by the Boltzmann distribution,  $W_\alpha$ , for ortho and para isomers independently:

$$\rho_{\alpha\alpha} = \rho_o W_\alpha; \quad \rho_{\alpha'\alpha'} = \rho_p W_{\alpha'}, \quad (10)$$

because the rotational relaxation inside the ortho and para subspaces is many orders of magnitude faster than the ortho-para conversion. In Eq.(10)  $\rho_o$  and  $\rho_p$  are the total concentrations of ortho and para molecules, respectively. The Boltzmann factors are determined in the standard way by the expression

$$W_\alpha = Z_{ortho}^{-1} \exp(-E_\alpha/kT), \quad (11)$$

for the ortho molecules and similarly for para. In (11),  $E_\alpha$  is the energy of state  $\alpha$ ;  $Z_{ortho}$  and  $Z_{para}$  are the partition functions for ortho and para molecules, respectively.

Let us represent  $\rho_o$  as the sum of a steady-state and a time-dependent part:  $\rho_o = \bar{\rho}_o + \delta\rho_o(t)$ . By taking into account that the total molecular concentration  $N = \rho_o + \rho_p$  is conserved, one finds from (9) and (10) an exponential decay:

$$\delta\rho_o(t) = \delta\rho_o(0)e^{-\gamma t}, \quad (12)$$

with the conversion rate

$$\gamma = \sum_{\alpha \in o, \alpha' \in p} \frac{2\Gamma |V_{\alpha\alpha'}|^2}{\Gamma^2 + \omega_{\alpha\alpha'}^2} (W_{\alpha'} + W_{\alpha}). \quad (13)$$

This expression gives the solution to the problem in first order perturbation theory. It is valid for not too strong mixing, such that

$$|V|^2 \ll \frac{\nu_{rot}}{4\Gamma} \max\{\Gamma^2, \omega^2\}, \quad (14)$$

where  $\nu_{rot}$  is the rotational relaxation rate. Conversion in the more general case is considered in [35].

## 2.2 Ortho-para state mixing in $CH_3F$

The model of spin conversion described above is simple and clear, but is there something inside a symmetrical molecule which mixes the ortho and para states? We know now that such mixing can be produced by hyperfine interactions. These interactions are very weak and usually show up as small effects on a much larger background. Quantum relaxation of spin isomers provides an example of a phenomenon for which hyperfine interactions are the leading force.

Hyperfine interactions in molecules are important for various physical problems, first of all for hyperfine spectroscopy. We note that for the nuclear spin conversion one needs a specific part of hyperfine interaction which mixes the ortho and para states. This part of hyperfine interaction is unimportant for standard hyperfine spectroscopy but is important for level crossing/anticrossing spectroscopy (see Ref. [43] and references therein).

Let us recall the classification of  $CH_3F$  quantum states. As a consequence of the  $CH_3F$  symmetry the molecules exist in form of two nuclear spin isomers: ortho and para which have a total spin of three hydrogen nuclei  $I = 3/2$  and  $I = 1/2$ , respectively (see, for example [44]). The ortho molecules have  $K$ -values ( $K$  refers to the angular momentum projection on the molecular symmetry axis)

divisible by 3:  $K = 0, 3, 6 \dots$ . For para isomers only  $K = 1, 2, 4, 5 \dots$  are allowed. Consequently, the quantum states of  $\text{CH}_3\text{F}$  are divided into two subspaces, ortho and para, which are shown in Figure 1 for the particular case of  $^{13}\text{CH}_3\text{F}$  molecules.

An analysis of ortho-para mixing in  $\text{CH}_3\text{F}$  in relation with the spin conversion problem was performed in a few papers. Two sources of mixing in  $\text{CH}_3\text{F}$  have been considered so far: spin-spin interactions between the molecular nuclei [45, 46, 47] and spin-rotation interactions [46, 47, 48, 49, 50].

Spin-spin interactions. The ortho and para states in  $\text{CH}_3\text{F}$  are mixed by spin-spin interaction between the three hydrogen nuclei ( $\hat{V}_{HH}$ ), the fluorine-hydrogen nuclei ( $\hat{V}_{FH}$ ) and the carbon-hydrogen nuclei ( $\hat{V}_{CH}$ ) in the case of  $^{13}\text{CH}_3\text{F}$  (see Figure 2). These interactions can be written as

$$\begin{aligned}\hat{V}_{HH} &= P_{HH} \sum_{m < n} \hat{\mathbf{I}}^{(m)} \hat{\mathbf{I}}^{(n)} \bullet \mathbf{T}^{(m,n)}; & \hat{V}_{FH} &= P_{FH} \sum_m \hat{\mathbf{I}}^{(m)} \hat{\mathbf{I}}^F \bullet \mathbf{T}^{mF}; \\ \hat{V}_{CH} &= P_{CH} \sum_m \hat{\mathbf{I}}^{(m)} \hat{\mathbf{I}}^C \bullet \mathbf{T}^{mC},\end{aligned}\quad (15)$$

with  $m, n = 1, 2, 3$  denoting the protons. In (15)  $P$  are scale factors having the order of magnitude  $10^4$  Hz. Their numerical values are given in [45];  $\hat{\mathbf{I}}$  are the spin operators of the corresponding nuclei;  $\mathbf{T}$  are the second rank tensors for the magnetic dipole-dipole interaction having the form, e.g.,

$$T_{ij}^{mF} = \delta_{ij} - 3n_i^{mF} n_j^{mF}, \quad (16)$$

where  $\mathbf{n}^{mF}$  is the unit vector directed from the  $\text{H}^{(m)}$  to the F nucleus.

The spin conversion rate in  $^{13}\text{CH}_3\text{F}$  molecules induced by the spin-spin interactions  $\hat{V}^{SS} = \hat{V}_{HH} + \hat{V}_{FH} + \hat{V}_{CH}$ , is given by the expression (13) having a mixing efficiency for the ortho-para level pair  $(J', K')-(J, K)$  [45]

$$\begin{aligned}\sum |V_{\alpha\alpha'}^{SS}|^2 &\equiv F_{SS}(J', K'|J, K) = (2J' + 1)(2J + 1) \begin{pmatrix} J' & 2 & J \\ -K' & q & K \end{pmatrix}^2 \times \\ &\quad \left( 3 |P_{HH} \mathcal{T}_{2q}^{(1,2)}|^2 + 2 |P_{FH} \mathcal{T}_{2q}^{1F}|^2 + 2 |P_{CH} \mathcal{T}_{2q}^{1C}|^2 \right).\end{aligned}\quad (17)$$

Here  $\mathcal{T}$  are the spherical components of the corresponding  $\mathbf{T}$ -tensors calculated in the molecular frame (for their numerical values see [45]);  $(: : :)$  stands for the 3-j symbol. In the left-hand side of (17) summation is performed over degenerate quantum numbers of the states  $\alpha$  and  $\alpha'$  which are the projections on the laboratory quantization axis of molecular angular momentum  $M$ , spins  $\sigma$ ,  $\sigma^F$ ,  $\sigma^C$  of the three protons, fluorine and carbon nucleus, respectively.

The selection rule for the spin-spin mixing follows from Eq.(17):

$$|\Delta J| \leq 2; \quad J' + J \geq 2; \quad |\Delta K| \leq 2. \quad (18)$$

Note that mixing of states having  $|\Delta K| = 0$  does not contribute to the spin conversion. By contrast, the level shift in hyperfine spectroscopy is dominated by the diagonal matrix elements of  $\hat{V}$  having  $|\Delta K| = 0$ .

The spin-spin interaction in  $\text{CH}_3\text{F}$  can be determined with rather high accuracy, limited presently to a few percent by the uncertainty in the molecular spatial structure. The most accurate data for the  $\text{CH}_3\text{F}$  structure are given in Ref. [51].

Spin-rotation interaction. Another source of ortho-para mixing in  $\text{CH}_3\text{F}$  is the spin-rotation coupling which results from the interaction of the nuclear spins with the magnetic field induced by molecular rotation [46, 47, 48, 49, 50]. The spin-rotation perturbation relevant for the ortho-para mixing can be written as [50]

$$\hat{V}_{SR} = \frac{1}{2} \sum_n [\hat{\mathbf{J}} \cdot \mathbf{C}^{(n)} \cdot \hat{\mathbf{I}}^{(n)} + H.C.], \quad (19)$$

where  $\mathbf{C}^{(n)}$  is the spin-rotation tensor for the  $n$ -th hydrogen nucleus. The expression for the ortho-para mixing efficiency due to the spin-rotation interaction can be found in the original papers [46, 47, 48, 49, 50].

The selection rules for the spin-rotation interaction read

$$|\Delta J| \leq 1; \quad |\Delta K| \leq 2. \quad (20)$$

As can be seen from the selection rules (18) and (20), there are ortho-para level pairs which are mixed exclusively by spin-spin but not by spin-rotation interaction, viz.,  $|\Delta J| = 2$ . This can be used to disentangle the contribution to the spin conversion from these two mechanisms of state mixing [49].

In contrast to spin-spin interaction, the spin-rotation interaction in  $\text{CH}_3\text{F}$  is known presently only approximately. It was proposed [46, 49] to use nuclear spin conversion itself as a source of information on spin-rotation perturbation in molecules. Such information would be complementary to the information provided by standard hyperfine spectroscopy.

### 2.3 $\text{CH}_3\text{F}$ level structure and theoretical conversion rates

Spin conversion by quantum relaxation is dependent on the position of ortho and para states, notably the ortho-para level gaps. They are not accessible di-

rectly by standard spectroscopical methods. Nevertheless, if a complete set of molecular parameters is available one can calculate the positions of all states and thus the ortho-para level gaps. The accuracy of the molecular parameters should be rather high to guarantee the determination of the level position within 1 – 10 MHz because only close ortho-para level pairs contribute substantially to the conversion. For CH<sub>3</sub>F such accurate parameters are available from high-resolution spectroscopy [52, 53, 54, 55, 34].

A search for close ortho-para level pairs in CH<sub>3</sub>F was performed in [45]. At the time, a complete set of ground state molecular parameters was available for <sup>12</sup>CH<sub>3</sub>F only [52]. For <sup>13</sup>CH<sub>3</sub>F the molecular parameters  $A_0$  and  $D_0^K$  were missing. Nevertheless, a search for close ortho-para level pairs was performed for both molecules using the estimation of  $A_0=5.18240(6)$  cm<sup>-1</sup> made by T Egawa and K Kuchitsu (unpublished data) and assuming  $D_0^K$  equal for both isotopes. This search revealed that only two ortho-para level pairs are important for the spin conversion in <sup>13</sup>CH<sub>3</sub>F. For <sup>12</sup>CH<sub>3</sub>F four important ortho-para level pairs were found. This choice of level pairs was confirmed and their energy gaps determined more precisely in [56] on the basis of new accurate molecular parameters determined in [54, 55]. The best presently available values for the CH<sub>3</sub>F ortho-para level gaps are given in Table 1.

In addition to the ortho-para level spacing,  $\omega_{\alpha\alpha'}$ , and the efficiency of the ortho-para mixing,  $V_{\alpha\alpha'}$ , the decoherence rate,  $\Gamma$ , should be determined in order to calculate the conversion rates. This is a rather complicated problem that has not yet been resolved. Approximately, the rate  $\Gamma$  can be taken equal to the level population decay rate. Even so, the uncertainty remains because the population decay rates of the states important for the conversion (see Table 1) have not been measured. There is a measurement of the population decay rate in the state ( $J=4, K=3$ ) of <sup>13</sup>CH<sub>3</sub>F [57] which was determined to be  $1\cdot 10^8$  s<sup>-1</sup>/torr.

Since the decoherence rate  $\Gamma$  is close to but nevertheless different from the level population decay rate, it is more consistent to determine  $\Gamma$  from the nuclear spin conversion itself by fitting the measured conversion rate. Such an approach [58, 59] yields  $\Gamma \simeq 1.8\cdot 10^8$  s<sup>-1</sup>/torr which is indeed close to the level population decay rate  $1\cdot 10^8$  s<sup>-1</sup>/torr [57]. The various mixing processes in CH<sub>3</sub>F are illustrated in Table 1 where the contributions to the conversion are calculated assuming the

decoherence decay rate  $\Gamma = 1.8 \cdot 10^8 \text{ s}^{-1}/\text{torr}$  for all pairs of ortho-para states in both molecules.

From the data in Table 1 one can see that the conversion in  $^{12}\text{CH}_3\text{F}$  by spin-spin interaction is much slower than in  $^{13}\text{CH}_3\text{F}$ . On the other hand, in  $^{12}\text{CH}_3\text{F}$  the spin-rotation interaction was predicted to be the leading mechanism [60, 50]. The key point is the right choice of the decoherence rate  $\Gamma$  for the most important level pair in  $^{12}\text{CH}_3\text{F}$ : (28,5)-(27,6). It was proposed in [50] to use  $\Gamma \simeq 2 \cdot 10^7 \text{ s}^{-1}/\text{torr}$  for this pair in order to fit the experimental value for the rate.

### 3 EXPERIMENTAL METHOD

#### 3.1 Spin isomer separation by LID

It is the introduction of the Light-Induced Drift (LID) [29] as a separation tool that has brought substantial progress in the field of nuclear spin isomers over the last decade. The essence of LID is explained in Figure 3. Let us consider a gas of two-level particles interacting with a traveling monochromatic wave. Due to the Doppler effect, the radiation will excite particles selectively with respect to their velocity component along the radiation  $\mathbf{k}$ -vector.

Suppose that the absorbing particles are diluted in a buffer gas and that the laser frequency is chosen such that the radiation excites only molecules moving away from the laser. Because the excited molecules have in general a different (usually bigger) kinetic cross section than the unexcited particles, the mean free path for molecules moving away from the laser will be different (usually smaller) than for molecules moving towards the laser. This difference in mean free path will create a drift of absorbing particles towards the laser. The buffer gas will flow in the opposite direction as required by momentum conservation. The direction of the fluxes depends on the sign of the laser frequency detuning from the absorption line center and the direction of the wave vector  $\mathbf{k}$ . In a closed tube the LID effect results in a spatial separation of the two gas components, which can be quite substantial even if the fluxes themselves are relatively small.

A quantitative description of the LID effect in molecules is a complicated problem because LID depends on small difference in transport properties between excited and ground state molecules, which is rather difficult to calculate. A crucial

parameter is the relative change in cross section, or – more precisely – in collision rate,  $\Delta\nu/\nu$ , upon excitation. In general,  $\Delta\nu/\nu$  depends on velocity, and thus on the detuning. In some cases  $\Delta\nu/\nu$  can even change sign as a function of detuning, giving rise to so called “anomalous LID” (see, e.g., Refs. [62]). Here we will limit ourselves to the simplified case that  $\Delta\nu/\nu$  can be considered constant. In this case the description of LID is relatively simple [63] and yields for the difference in absorbing particle density between the ends of the tube

$$\Delta n = -\frac{\Delta\nu}{\nu} \frac{2\Delta S}{\hbar\omega v_0} \varphi(\Omega), \quad (21)$$

where  $\Delta S$  is the absorbed laser intensity;  $\hbar\omega$  is the photon energy;  $v_0 = \sqrt{2kT/m}$  is the thermal speed;  $\varphi(\Omega)$  describes the behavior as a function of detuning,  $\Omega = \omega - \omega_0$ , of the laser frequency,  $\omega$ , from the absorption line center frequency,  $\omega_0$ . The spectral function  $\varphi(\Omega)$  can be readily calculated if the homogeneous line width of the absorbing transition is known. For small frequency detuning and low pressure, the function  $\varphi(\Omega) \simeq v_L/v_0$ , where  $v_L = \Omega/k$  is the resonant velocity component of the absorbing particle along the  $\mathbf{k}$ -vector. Examples of  $\varphi(\Omega)$  for various homogeneous line widths, as well as corrections to (21) due to the finite gas dilution are given in [64].

It was shown in Ref. [65] that the LID effect in the  $\text{CH}_3\text{F}$  isotope mixture, which should behave similar to the mixture of spin isomers, is consistent with the model of constant  $\Delta\nu/\nu$ . The change in collision rate,  $\Delta\nu/\nu$ , upon rovibrational excitation was found to be  $\simeq 1\%$ . For more details on the LID effect see Ref. [66] and Refs.[65, 67] which review the LID effect in molecular gases.

A prerequisite of the LID separation of gas components is their spectral distinguishability. This is perfectly satisfied for  $\text{CH}_3\text{F}$  for which ortho and para isomers are different by  $K$  and thus have different absorption spectra. There are two convenient coincidences between absorption lines of  $^{13}\text{CH}_3\text{F}$  and  $^{12}\text{CH}_3\text{F}$  molecules in the  $\nu_3$  fundamental band (C–F stretch) and  $\text{CO}_2$ -laser lines [68], which were used for spin isomer separation. The absorption spectra of ortho and para  $^{13}\text{CH}_3\text{F}$  near the P(32) line of the  $9.6 \mu$  band of a  $\text{CO}_2$ -laser are shown in Figure 4. As can be seen from these spectra, the  $\text{CO}_2$ -laser frequency tuned to the center of the 9P(32) laser line excites ortho  $^{13}\text{CH}_3\text{F}$  molecules in the blue wing of the R(4,3). This results in LID of ortho isomers towards the laser. In the case of  $^{12}\text{CH}_3\text{F}$ , excitation of the molecular absorption line Q(12,2) by the

9P(20) laser line induces a drift of para molecules away from the laser. In a typical experiment on CH<sub>3</sub>F spin isomer an enrichment of 10% was produced, sufficient to have good signal-to-noise ratio.

### 3.2 Relaxation time measurement

The experiments on CH<sub>3</sub>F were performed in Novosibirsk and Leiden using similar approaches. Separation of spin isomers was achieved in a long and thin glass tube using LID as outlined in Section 3.1. One end of the separation tube was connected with a test cell to collect an enriched gas sample. The other end of the separation tube was connected with a ballast volume, thus providing an equilibrium reference sample (see Figures 5 and 6). The degree of enrichment (or depletion, depending on the particular arrangement) was monitored by absorption, using a probe laser beam resonant with either the ortho, or the para isomer. To increase the sensitivity and stability of the detection system the absorption in the test cell was compared differentially with the absorption in a reference cell having equilibrium composition.

A schematic of the setup used in Ref. [33] is presented in Figure 5. The isomer separation was performed in a tube having length 1.5 m and inner diameter 1.3 mm by CO<sub>2</sub>-laser radiation (power  $\simeq 10$  W). The radiation frequency was stabilized to the CO<sub>2</sub> line center. For the enrichment detection, a small portion of the laser beam was directed through the test and reference cells which were placed on the same optical axis. The absorption in these cells was modulated in antiphase by external Stark electrodes. This modulation produced a component in the probe beam proportional to the absorption difference between the two cells. This differential signal was normalized by the signal proportional to probe beam intensity. The latter signal was created by additional Stark electrodes which modulated the absorption in the reference cell alone. The detection method used in [33] has a rather high sensitivity but has the drawback that it can be applied to molecules having permanent electric dipole moment only.

The setup used in Ref. [40] is presented in Figure 6. It has a separation tube of 30 cm length and 3 mm inner diameter for the study of <sup>13</sup>CH<sub>3</sub>F. For <sup>12</sup>CH<sub>3</sub>F a tube of 1 m length and 1.1 mm diameter was used to make up for the much smaller absorption of the  $Q(12,2)$  transition used. In both cases the separation laser (a



CO<sub>2</sub> laser from Edinburgh Instrument, Model PL5) was frequency stabilized to the CO<sub>2</sub>-line center.

For the detection, a weak probe beam from an additional (waveguide) laser was used. Intensity and direction of the beam were stabilized using an Acousto Optic Modulator with a feed back loop and a set of diaphragms. The frequency was locked to the CH<sub>3</sub>F absorption line center using an additional absorption cell with CH<sub>3</sub>F gas at low pressure.

It is essential to be sure that the powerful CO<sub>2</sub> laser radiation indeed produces separation of CH<sub>3</sub>F spin isomers and that spurious effects like gas heating, laser induced thermal diffusion, etc., do not contribute substantially to the signal. This important issue was addressed already in the first experiment, where the spin isomer separation was confirmed by comparing the optical signal with additional monitoring of the gas composition by a mass-spectrometer. A more decisive test was performed in [69] where it was demonstrated, by probing various ortho and para absorption lines, that the LID enrichment of ortho is accompanied by a corresponding depletion of para species. We stress that the conversion of spin isomers takes place in a part of the setup which is unaffected by the strong laser beam used for the isomer separation.

Depending on the problem at hand, the test cell could be connected to a Stark cell, or to a cell at elevated temperature, or to a cell containing different test surfaces. This allowed to study the influence of various physical factors on nuclear spin conversion.

The measurement procedure was generally as follows. First, the setup was filled with equilibrium gas and the detection system was set to zero absorption difference. Next, the enrichment was started by switching on the separation laser (first part of the curve in Figure 7). After a sufficient enrichment was achieved, the two probe cells were isolated by closing the appropriate valves and the conversion process began (the decay part in Figure 7). The measured decay curve was fitted by a function  $\exp(-\gamma t) + \kappa t$ , where  $\gamma$  is the conversion rate, while the second term accounts for a (small) drift of the detection signal.

## 4 EXPERIMENTAL RESULTS

#### 4.1 Dependence on pressure and collision partner

In the following Sections we review the experiments which test the mechanism responsible for spin conversion in CH<sub>3</sub>F. Let us first consider the pressure dependence. The data for <sup>13</sup>CH<sub>3</sub>F conversion in two buffer gases, <sup>12</sup>CH<sub>3</sub>F and <sup>13</sup>CH<sub>3</sub>F itself are shown in Figure 8. The rates have linear pressure dependence and are seen to be rather close. As the reference value we give the conversion in pure <sup>13</sup>CH<sub>3</sub>F [41]

$$\gamma_{13}/P = (12.2 \pm 0.6) \cdot 10^{-3} \text{ s}^{-1}/\text{torr}, \quad (22)$$

where the subscript 13 refers to the isotopic species.

The linear pressure dependence of  $\gamma_{13}$  is consistent with conversion by quantum relaxation. Indeed, at  $P \simeq 1$  torr the decoherence rate  $\Gamma/2\pi \simeq 30$  MHz, which is much smaller than the frequency gaps between the mixed states in <sup>13</sup>CH<sub>3</sub>F (see Table 1). In this pressure limit, where  $\Gamma \ll \omega$ , one can neglect  $\Gamma^2$  in the denominator of Eq.(13) and the conversion rate becomes proportional to  $\Gamma$ , thus proportional to pressure.

Note that the linear pressure dependence of  $\gamma_{13}$  at low pressures in itself does not allow to distinguish between conversion by quantum relaxation and by ordinary gaseous relaxation. The latter would produce conversion with a rate  $2n\sigma(p|o)v$  which is also linear in pressure (see Section 5.2). The important point is that quantum relaxation is able to reproduce the right order of magnitude for the conversion rate in <sup>13</sup>CH<sub>3</sub>F [45]. If one takes as an estimation for the decoherence rate  $\Gamma = 1 \cdot 10^8 \text{ s}^{-1}/\text{torr}$ , as follows from measurement [57], the spin-spin mixing of states in <sup>13</sup>CH<sub>3</sub>F gives the conversion rate  $\gamma_{13}/P \simeq 7 \cdot 10^{-3} \text{ s}^{-1}/\text{torr}$  which is half the measured value.

Measurements of the <sup>13</sup>CH<sub>3</sub>F spin conversion in various buffer gases are presented in Figure 9 [40, 41]. The conversion rates are rather close in buffer gas CH<sub>3</sub>Cl and in pure CH<sub>3</sub>F but are much smaller in buffer gases N<sub>2</sub> and O<sub>2</sub>. As was concluded in [40, 41], the buffer gas dependence of the conversion rate is in qualitative agreement with the buffer gas variation of the decoherence rate,  $\Gamma$ , which was estimated in [40, 41] on the basis of pressure broadening data. An important result of the data in Figure 9 is that the large magnetic moment of O<sub>2</sub> ( $\simeq 2 \mu_B$ ) seems to be unimportant for the <sup>13</sup>CH<sub>3</sub>F spin conversion. For more details on this point see Section 5.

#### 4.2 Isotope effect

The measurements show a large isotope effect in CH<sub>3</sub>F conversion [33, 59]. In Figure 10 the <sup>12</sup>CH<sub>3</sub>F conversion rate as a function of pressure is presented and seen to be much smaller than for <sup>13</sup>CH<sub>3</sub>F (Figure 8). The ratio of the conversion rates in <sup>13</sup>CH<sub>3</sub>F and <sup>12</sup>CH<sub>3</sub>F measured in Leiden [59] was found to be

$$\gamma_{13}/\gamma_{12} = 55 \pm 4, \quad (23)$$

which is close to the value  $46 \pm 5$  measured in [33]. The slow conversion rate in <sup>12</sup>CH<sub>3</sub>F makes the measurements rather difficult to perform because of severe restrictions to the long term stability of the detection system.

The much smaller rate in <sup>12</sup>CH<sub>3</sub>F results from the bigger gaps between the ortho and para states in this molecule in comparison with <sup>13</sup>CH<sub>3</sub>F. There is one close pair of ortho-para states, viz., (51,4)-(50,6), but these states are situated at high energies and therefore hardly populated. The <sup>13</sup>CH<sub>3</sub>F conversion is dominated by spin-spin mixing of the ortho and para states. In <sup>12</sup>CH<sub>3</sub>F the spin-spin interaction gives only a small part of the observed rate [56]. As was discussed in Section 2.3 and concluded in the papers [60, 50] the conversion in <sup>12</sup>CH<sub>3</sub>F is dominated by spin-rotation interaction.

#### 4.3 Temperature dependence

The levels important for spin conversion in <sup>13</sup>CH<sub>3</sub>F and <sup>12</sup>CH<sub>3</sub>F are situated at widely different energies. Consequently, one would expect quite different temperature dependences of the rates in the two cases as the level populations will be affected differently by temperature. For example, the population of the states (11,1) and (9,3), which are dominant for <sup>13</sup>CH<sub>3</sub>F conversion, will decrease at elevated temperature, in contrast with, e.g., states (51,4) and (50,6) of <sup>12</sup>CH<sub>3</sub>F whose population will increase.

The temperature dependence of the conversion rate in the two molecules was reported in Ref. [59]. The results of the measurements are presented in Figure 11. Indeed, the conversion rate in <sup>12</sup>CH<sub>3</sub>F grows rapidly with increasing temperature. By contrast, the rate in <sup>13</sup>CH<sub>3</sub>F decreases in the temperature range 300 - 600 K.

Presently we can propose only a rough model of the temperature dependence. The conversion rates is affected primarily through the Boltzmann occupation of

rotational states. An additional temperature dependence may appear due to the temperature dependence of the decoherence rate  $\Gamma$ . It proved sufficient to apply only a 25% temperature variation in  $\Gamma$  by the expression:

$$\Gamma(T) = \left(1.8 - (T - T_{room}) \cdot 1.5 \cdot 10^{-3} K^{-1}\right) \cdot 10^8 s^{-1}/torr, \quad (24)$$

to fit the experimental points for the  $^{13}\text{CH}_3\text{F}$  conversion in the range from room temperature  $T_{room}=297$  K up to 600 K, as shown by the thick line in Figure 11. Thus these data are qualitatively consistent with spin conversion by quantum relaxation (for  $T \geq 600$  K see below).

The same temperature dependence of the decoherence rate  $\Gamma(T)$  was used to model the conversion in  $^{12}\text{CH}_3\text{F}$ . Again, only spin-spin mixing of states was taken into account. The calculated rate in  $^{12}\text{CH}_3\text{F}$  (thin line) reproduces the overall behavior but fails to reproduce the magnitude of the rate. This may not be surprising, since an additional contribution to the conversion rate in  $^{12}\text{CH}_3\text{F}$  should result from spin-rotation interaction, as was pointed out in [60, 50].

Above 600 K the conversion rate in  $^{13}\text{CH}_3\text{F}$  increases again, which suggests an additional conversion mechanism at high temperatures. This mechanism seems to have no isotope selectivity, as one may conclude from Figure 11.

#### 4.4 Level-crossing resonances

Eq.(13) predicts a strong dependence of the conversion rate on ortho-para level spacing at low pressures where  $\Gamma \ll \omega$ . To detect this effect, it was proposed [61] to split and cross the ortho and para levels of  $^{13}\text{CH}_3\text{F}$  by a homogeneous electric field. This experiment was performed in [58] with the setup in Figure 6 equipped with an additional Stark cell.

Results of the measurement of the conversion rate in  $^{13}\text{CH}_3\text{F}$  as a function of electric field are shown in Figure 12. As seen from these data the conversion rate is hardly affected by the field below 500 V/cm, but rises sharply above 600 V/cm.

A theoretical description of the level-crossing resonances presented in Figure 12 was developed in [61, 58]. A homogeneous electric field splits each state of  $\text{CH}_3\text{F}$  into  $2J + 1$  magnetic sublevels due to the first order Stark effect. The energy gaps between the  $M$ -sublevels of the two states  $|J', K', M' \rangle$  and  $|J, K, M \rangle$

are given by the formula [44]

$$\hbar\omega_{M'M}(\mathcal{E}) = \hbar\omega_0 - \mathcal{E}d \left( \frac{M'K'}{J'(J'+1)} - \frac{MK}{J(J+1)} \right), \quad (25)$$

where  $\hbar\omega_0$  is the energy gap between the states  $|J', K' \rangle$  and  $|J, K \rangle$  at zero electric field;  $\mathcal{E}$  is the electric field strength,  $d$  is the molecular electric dipole moment. For  $^{13}\text{CH}_3\text{F}$ ,  $d$  was taken to be 1.858 D (or  $6.198 \times 10^{-30}$  C·m) [68].

In the model of level-crossing spectra [61, 58] only spin-spin interaction was taken into account. In this case each ortho-para level pair gives the following “spectrum” of  $\gamma$  as a function of field strength:

$$\gamma(\mathcal{E}) = \sum_{M \in o, M' \in p} \frac{2\Gamma F_{SS}(J', K'|J, K)}{\Gamma^2 + \omega_{M'M}^2(\mathcal{E})} \left( \begin{array}{ccc} J' & J & 2 \\ -M' & M & M' - M \end{array} \right)^2 (W_{\alpha'} + W_{\alpha}), \quad (26)$$

where  $F_{SS}(J', K'|J, K)$  is the mixing efficiency from (17). The selection rule  $|\Delta M| \leq 2$  follows directly from (26). The only unknown parameter in expression (26) is the decoherence rate  $\Gamma$ . This parameter was determined in [58] by fitting the experimental value of  $\gamma$  in  $^{13}\text{CH}_3\text{F}$  at zero electric field which gave  $\Gamma \simeq 1.8 \cdot 10^8 \text{ s}^{-1}/\text{torr}$ .

Once  $\Gamma$  is determined, there are no free parameters in the model and the level-crossing spectra can be calculated. The result is presented in Figure 12. As can be seen from these data, the model reproduces the main features of the measured spectrum very well: positions of the peaks within a few MHz as well as their amplitude within 10%.

The spectrum in Figure 12 results from crossing of sublevels of the ortho state (9,3) and the para state (11,1). The level pair (21,1)-(20,3) gives a constant contribution to  $\gamma(\mathcal{E})$  in the electric field range of Figure 12 because of the much larger gap for this level pair: 350 MHz. The states (11,1) and (9,3) have  $\Delta J = 2$  and consequently are mixed by spin-spin interactions but not by spin-rotation interaction. This justifies taking only spin-spin interaction into account in the modeling of the level-crossing resonances [61, 58].

#### 4.5 Quantum Zeno effect induced by collisions

In the high pressure limit, where  $\Gamma \gg \omega$ , one can neglect  $\omega$  in the denominator of (13) and the conversion rate is seen to be inversely proportional to pressure (“1/P

dependence”). Consequently, at high pressures one has a very interesting regime of spin conversion in which rapid collisions prevent the molecule from changing its spin state: collisional inhibition of spin conversion. This slowing down of the conversion should start in the case of  $^{13}\text{CH}_3\text{F}$  at pressures well above 10 torr. Unfortunately it was not possible to perform measurements at such high pressures because of a few experimental problems. First, the LID effect is reduced at high pressures due to loss of velocity selectivity by pressure broadening. Second, the attained level of enrichment at high pressures becomes smaller also because the diffusion-limited separation time increases whereas the spin relaxation time is rather short at 10 torr, making back-conversion during the enrichment stage more severe. Third, the sensitivity of the detection system decreases because of overlapping ortho and para absorption lines. Another approach to observe the slowing down of the conversion would be to enrich at low pressures and to increase the pressure afterwards. Such an attempt was unsuccessful mainly because of spurious effects accompanying the compression [69].

To overcome these problems one could, as an alternative, narrow the gap between the ortho and para levels by an external electric field. This would shift the slowing down of the conversion rate to lower pressures. The idea was realized in [70] by choosing the field strength at which the strongest peak in the spectrum of Figure 12 occurs. This peak is due to the crossing of sublevels  $M'=11$  and  $M=9$  at electric field 652.8 V/cm. If this resonant condition is chosen and the spin conversion is dominated by mixing of the resonant level pair, the description of the conversion is given by just one term from Eq.(26) which has  $\omega = 0$  in the denominator and gives a  $1/P$  dependence.

The result of the measurements is shown in Figure 13. Indeed, there is a rapid slowing down of the conversion rate when the pressure increases from 0.05 torr to 0.5 torr. The plateau above 0.5 torr is the result of the neighboring  $M' - M$  level pairs which do not have zero gaps at the chosen electric field and, consequently, give a contribution which is still increasing with pressure. At still higher pressures, the conversion rate would go down again.

The experimental results in the high pressure range are in good agreement with the theory (solid line in Figure 13). The calculation of the pressure dependence was performed on the basis of Eq.(26) by taking into account all pairs ( $J'=11$ ,

$K'=1, M')$ -( $J=9, K=3, M$ );  $|M' - M| \leq 2$ . The decoherence rate was taken to be  $\Gamma=1.75 \times 10^8 \text{ s}^{-1}/\text{torr}$  for all level pairs. Only the spin-spin mixing of states was taken into account because this pair of states has  $|\Delta J|=2$  and, consequently, is not mixed by the spin-rotation interaction, see (20).

At low pressure the theoretical conversion rates are systematically larger than the measured one. This can be attributed to the saturation effect which should occur at low pressure in case of degenerate ortho and para states when the first order perturbation theory breaks down [35, 71]

The inhibition of the conversion rate at increasing collision rate can be considered as an example of the Quantum Zeno effect [72]. In the original version of this effect [72] the inhibition of the quantum system decay is due to frequent measurements which destroy quantum coherence by projecting the system to a particular quantum state. In our case the decoherence is produced by molecular collisions which destroy the coherence between the ortho and para states in the molecule.

## 5 DIRECT ORTHO-PARA TRANSITIONS IN $\text{CH}_3\text{F}$

The investigation of nuclear spin conversion in  $\text{CH}_3\text{F}$  would not be complete without studying direct ortho-para transitions in this molecule, i.e., transitions caused by the magnetic-field gradient from a collision partner or a surface. There is room for the conversion by quantum relaxation only if direct transitions are unimportant. Below we describe the two “direct” contributions to the conversion which are produced by surface or bulk collisions.

### 5.1 *Direct conversion on surfaces*

For the case of ortho and para  $\text{H}_2$ , conversion on catalytic surfaces is by far the most efficient mechanism (see e.g. [8, 73, 74, 75]). This may not be surprising in view of the extremely slow gas-phase conversion. But also for  $\text{CH}_3\text{F}$ , conversion on surfaces plays a role. As was demonstrated in Refs.[31, 69],  $\text{CH}_3\text{F}$  nuclear spin conversion can be quite different for different wall materials. The most rapid conversion (in fact instantaneous on the experimental time scale) was observed on  $\text{Fe}(\text{OH})_3$  powder [31]. The rate of conversion on this catalyst was limited, most likely, by diffusion.

Glass surfaces appeared to be rather inert for the  $\text{CH}_3\text{F}$  conversion. The surface contribution to the conversion is given by a cutoff of the linear fit of the conversion rate vs. pressure. The data in Figure 8 determines the surface contribution on the order of  $10^{-4} \text{ s}^{-1}$ . This yields a probability per collision for the molecule to convert  $\simeq 10^{-9}$  [31, 69]. There are other surfaces which do not seem to produce rapid conversion, e.g., aluminum and gold. On the other hand, conversion on the surface of magnetic tape was found to be rather fast [69].

### 5.2 Direct conversion by collisions

Another possible mechanism of direct ortho-para transitions is due to collisions in the bulk. In the case of hydrogen, it is known [4] that oxygen molecules speed up hydrogen conversion dramatically, although in a time domain different from the  $\text{CH}_3\text{F}$  conversion. This phenomenon is well understood [76]. The conversion is due to the steep magnetic field gradient produced by the collision partner.

Conservation of the nuclear spin symmetry of symmetric tops in molecular collisions was confirmed in a number of studies using various experimental approaches [77, 78, 79, 80, 81, 82]. This is not surprising, because we know now that spin isomers are very stable species.

Nevertheless, it would be useful to know the conversion rate in direct collisions. First of all we would like to stress that conservation of nuclear spin symmetry in molecular collisions is an approximate selection rule, although a very precise one. Like in the case of hydrogen, it can be violated if an inhomogeneous magnetic field is produced by a colliding molecule. From the measurements of the  $\text{CH}_3\text{F}$  conversion rate one can estimate an upper bound for the cross section of direct spin-changing collisions  $\sigma(p|o)$ . Using the formula for the gas-kinetic relaxation rate  $\gamma_{coll} = 2N\sigma(p|o)v$  and the experimental value for the conversion rate  $0.01 \text{ s}^{-1}$  [33, 41] one obtains the estimation

$$\sigma(p | o) \leq 2.5 \cdot 10^{-24} \text{ cm}^2. \quad (27)$$

Cross sections of this order are hardly accessible by conventional collision experiments, like molecular beams, or double resonance techniques.

In order to reveal the role of the magnetic moment of the collision partner, the  $^{13}\text{CH}_3\text{F}$  spin conversion was studied in two buffer gases:  $\text{N}_2$  and  $\text{O}_2$  which



have quite similar pressure broadening coefficients and, consequently, should have similar contributions to the conversion due to quantum relaxation [41]. On the other hand, the magnetic moments of  $\text{N}_2$  and  $\text{O}_2$  are different by three order of magnitude, which can result in extra contribution to the conversion in the case of oxygen. From the data for  $^{13}\text{CH}_3\text{F}$  presented in Figure 9, one can conclude that the role of the oxygen magnetic moment is too small to be visible on the much larger background which is due to conversion by quantum relaxation. Thus in order to observe direct ortho-para transitions one has to suppress the contribution by quantum relaxation. It was proposed in [83] to search for spin-violating collisions by studying spin conversion in  $^{12}\text{CH}_3\text{F}$ , in which the conversion by quantum relaxation is slower by almost two orders of magnitude than in  $^{13}\text{CH}_3\text{F}$ .

The results of the measurements are presented in Figure 14. One can see that the  $^{12}\text{CH}_3\text{F}$  conversion is considerably faster in collisions with  $\text{O}_2$  than with  $\text{N}_2$ . The difference in rates can be attributed [83] to direct ortho-para transitions. The estimation for the cross section from the data in Figure 14 reads

$$\sigma(p|o) = (6 \pm 0.8) \cdot 10^{-26} \text{ cm}^2. \quad (28)$$

We see from this result that even if  $\text{CH}_3\text{F}$  is diluted in paramagnetic oxygen, the direct ortho-para transitions are very improbable if compared with ordinary kinetic cross sections. To understand to what extent the direct transition can influence the conversion in a “nonmagnetic” environment (like pure  $\text{CH}_3\text{F}$ ), one needs to scale the cross section  $\sigma(p|o)$  for the various magnetic moments. Similar to the case of hydrogen [76], the cross section of direct transitions for  $\text{CH}_3\text{F}$  scales with  $\mu^2$  where  $\mu$  is the magnetic moment of the collision partner [42]. Consequently, direct transitions can be neglected for  $\text{CH}_3\text{F}$  spin conversion in a nonmagnetic environment.

## 6 CONCLUSION

It is well established by now that the nuclear spin isomers of molecules can be separated in the gas phase by using the Light-Induced Drift technique. The enriched gas samples can be stored in a separate test volume for further investigations of their properties.

In the present review we have used  $\text{CH}_3\text{F}$  to investigate the mechanism behind

nuclear-spin conversion. This molecule was found to have conversion rates in a convenient time domain, and turned out to be very versatile for investigating various aspects of the conversion process. The conversion was studied at various pressures, temperatures and gas compositions and for two isotopic species. The experimental results obtained for the CH<sub>3</sub>F spin isomers revealed that the conversion in the bulk is governed by a specific process which can be called quantum relaxation. This mechanism is based on the intramolecular mixing of molecular quantum states and collisional destruction of the quantum coherence between the mixed states.

Various key points in the CH<sub>3</sub>F conversion by quantum relaxation were clarified. It includes, first of all, the knowledge of the most important levels in CH<sub>3</sub>F which contribute substantially to the conversion through mixing by intramolecular perturbations. Second, the mixing mechanism in <sup>13</sup>CH<sub>3</sub>F is shown to be the spin-spin interaction between the molecular nuclei. For <sup>12</sup>CH<sub>3</sub>F, on the other hand, there is evidence that the spin-rotation perturbation is the most important while spin-spin interactions play a minor role. Third, the decay rate of the coherence between ortho and para states by collisions in the bulk was determined experimentally. All these data gave an internally consistent picture of the spin conversion in CH<sub>3</sub>F.

The mechanism responsible for nuclear spin conversion in CH<sub>3</sub>F was tested experimentally in a few ways. The most decisive experiments are the observation of level-crossing resonances in the conversion rate and the observation of the slowing down of the conversion with increasing gas pressure (“Quantum Zeno Effect”).

Prospects for further development in the field of spin isomers look optimistic. Even if one restrict oneself to the spin isomers separation method based on LID, there is a large variety of investigations possible. The LID effect already proved to be an efficient separation tool for a number of molecules like NH<sub>3</sub>, C<sub>2</sub>H<sub>4</sub>, H<sub>2</sub>O which all have nuclear spin isomers. There is no doubt that investigations of molecular spin isomers similar to that for CH<sub>3</sub>F can be performed with various other molecules.

## **7 ACKNOWLEDGMENTS**

The results presented in this review were obtained in a long term project. We are indebted to many colleagues for fruitful and pleasant cooperation. More specifically, we would like to name the following colleagues (in the order in which they joined the project) V.N. Panfilov, V.P. Strunin, L.N. Krasnoperov, A.E. Bakarev, D. Papoušek, J Demaison, B. Nagels, M. Schuurman, D.A. Roozmond, N. Calas, P. Bakker, E. Ilisca, M. Irac-Astaud, K. Bahloul.

This project was made possible by financial support from the Netherlands Organization for Scientific Research (NWO), the Russian Academy of Sciences and the RFBR grant 98-03-33124a.

*Literature Cited*

1. Eucken A. 1912. Sitzber. Preuss. Akad. Wiss. 1912:41
2. Mecke R. 1925. Z. f. Physik. 31:709-712
3. Bonhoeffer KF, Harteck P. 1929. Naturwiss. 17:182
4. Farkas A. 1935. *Orthohydrogen, Parahydrogen and Heavy Hydrogen*. London: Cambridge University Press. 215 pp.
5. Cremer E. 1943. in *Handbuch der Katalyse 3*, Schwab GM, ed., Springer, Wien. p. 1
6. Trapnell BMW. 1955. in *Catalysis 3*, Emmett PH, ed., Reihold, New York, p. 1
7. Schmauch GE and Singleton AH. 1964. *Industrial and Engineering Chemistry* 56:20
8. Ilisca E. 1992. *Progress in Surface Science*. 41:217
9. Heitler W, Herzberg G. 1929. Naturwiss. 17:673-674
10. Bloom M. 1972. Nuclear spin relaxation in gases. In *MTP International Review of Science, Physical Chemistry Series, Magnetic Resonance*, ed. CA McDowell, 4:1-42. London/Baltimore: Butterworth/University Park Press. 365 pp.
11. Landau LD, Lifshitz EM. 1977. *Quantum Mechanics*, 3rd ed. Pergamon Press, Oxford. 673 pp.
12. Curl RF, Jr, Kasper JVV, Pitzer KS, Sathianandan K. 1966. *J. Chem. Phys.* 44:4636-4637
13. Curl RF, Jr, Kasper JVV, Pitzer KS. 1967. *J. Chem. Phys.* 46:3220-3228
14. Ozier I, Yi P-n. 1967. *J. Chem. Phys.* 47:5458-5459
15. Amrein A, Quack M, Schmitt U. 1988. *J. Mol. Spectrosc.* 92:5455-5466
16. Hepp M, Winnewisser G, Yamada KMT. 1994. *J. Mol. Spectrosc.* 164:311-314
17. Georges R, Herman M, Hilico JC, Roberto O. 1998. *J Mol. Spectrosc.* 187:13-20
18. Balykin VI, Letokhov VS, Mishin VI, Semchishen VA. 1976. *Chem. Phys.* 17:111-121
19. Booth JL, Dalby FW, Parmar S, Vanderlinder J. 1989. *Chem. Phys.* 132:209-217
20. Schramm B, Bamford DJ, Moor CB. 1983. *Chem. Phys. Lett.* 98:305-309
21. Kern J, Schwahn H, Schramm B. 1989. *Chem. Phys. Lett.* 154:292-298
22. Weber HG, Stock M. 1974. *Physics Letters*, A50:343-343
23. Bernheim RA, He Chun. 1990. *J. Chem. Phys.* 92:5959-5962
24. Konyukhov VK, Prokhorov AM, Tikhonov VI, Faizulaev VN. 1986. *Pis'ma Zh. Eksp. Teor. Fiz.* 43:65-67 [JETP Lett. 43:85-89]
25. Konyukhov VK, Tikhonov VI, Tikhonova TL. 1988. *Proceedings of Physical Institute of The USSR Academy of Sciences, (Kratkie Soobshcheniya po Fizike)*. 9:12-14 p.12
26. Quack M. 1977. *Mol. Phys.* 34:477-504
27. Uy D, Cordonnier M, Oka T. 1997. *Phys. Rev. Lett.* 78:3844-3847
28. Krasnoperov LN, Panfilov VN, Strunin VP, Chapovsky PL. 1984. *Pis'ma Zh. Eksp. Teor. Fiz.* 39:122-144 [JETP Lett. 39:143-146]
29. Gel'mukhanov FKh, Shalagin AM. 1979. *Pis'ma Zh. Eksp. Teor. Fiz.* 29:773-776 [JETP Lett. 29:711-713]
30. Panfilov VN, Strunin VP, Chapovsky PL. 1983 *Zh. Eksp. Teor. Fiz.* 85:881-892 [Sov. Phys.

- JETP 58:510-516]
31. Chapovsky PL, Krasnoperov LN, Panfilov VN, Strunin VP. 1985. Chem. Phys. 97:449-455
  32. Bakarev AE, Chapovsky PL. 1986. Pis'ma Zh. Eksp. Teor. Fiz. 44:5-6 [JETP Lett. 44:4-6]
  33. Chapovsky PL. 1990. Zh. Eksp. Teor. Fiz. 97:1585-1596 [Sov. Phys. JETP. 70:895-901]
  34. Papoušek D, Demaison J, Wlodarczak G, Pracna P, Klee S, Winnewisser M. 1994. J. Mol. Spectr. 164:351-367
  35. Chapovsky PL. 1996. Physica A (Amsterdam) 233:441-448
  36. Bloembergen N. 1961. *Nuclear Magnetic Relaxation*, W.A.Benjamin, Inc., New York. 178 pp.
  37. Orr BJ. 1995. Chem. Phys. 190:261-278
  38. Salikhov KM, Molin YuN, Sagdeev RZ, Buchachenko AL. 1984. *Spin Polarization and Magnetic Effects in Radical Reactions*, Elsevier, Amsterdam. 419 pp
  39. Feynman RP, Leighton RB, Sands M. 1963. *The Feynman Lectures in Physics*, Addison-Wesley Pub. Com. Ltd.
  40. Nagels B, Schuurman M, Chapovsky PL, Hermans LJF. 1995. J. Chem. Phys. 103:5161-5163
  41. Nagels B, Schuurman M, Chapovsky PL, Hermans LJF. 1996. Phys. Rev. A54:2050-2055
  42. Chapovsky PL. 1996. Chem. Phys. Lett. 254:1-5
  43. Ozier I, Meerts WL. 1981. Can. J. Phys. 59:150-171
  44. Townes CH, Shawlow AL. 1955. *Microwave Spectroscopy*, McGraw-Hill Publ. Comp., New York. 698 pp.
  45. Chapovsky PL. 1991. Phys. Rev. A43:3624-3630  
Chapovsky PL. 1991. "Light induced drift: application to nuclear spin modification problem," *Atomic Physics 12*, edited by J.C.Zorn and R.R.Lewis, AIP Conference Proceedings, AIP, New York. 233:504-518
  46. Gus'kov KI. 1995. Zh. Eksp. Teor. Fiz. 107:704-731 [JETP. 80:400-414]
  47. Bahloul K. 1998. *Des Interactions Hyperfines et de la Conversion des Isomères de Spin Nucléaire de CH<sub>3</sub>F*, Ph.D.Thesis. Univ. Paris-7, Denis Diderot. 249 pp.
  48. Chapovsky PL. 1997. "Nuclear spin conversion in molecules induced by hyperfine interactions," in 12th Symposium and School on High-Resolution Molecular Spectroscopy, Sinitsa LN, Ponomarev YuN, Perevalov VI, Editors, Proc. SPIE 3090:2-12
  49. Bahloul K, Irac-Astaud M, Ilisca E, Chapovsky PL. 1998. J. Phys. B.: At. Mol. Opt. Phys. 31:73-85
  50. Ilisca E, Bahloul K. 1998. Phys. Rev. A57:4296-4300
  51. Egawa T, Yamamoto S, Naketa M, Kuchitsu K. 1987. J. Mol. Structure. 156:213-228
  52. Graner G. 1976. Mol. Phys. 31:1833-1843
  53. Lee SK, Schwendeman RH, Crownover RL, Skatrud DD, and Delucia FC. 1987. J. Mol. Spectrosc. 123:145-160
  54. Papoušek D, Hsu Yen-Chu, Chen Hann-Sen, Pracna P, Klee S, Winnewisser M. 1993. J. Mol. Spectr. 159:33-41
  55. Papoušek D, Papoušková D, Hsu Yen-Chu, Pracna P, Klee S, Winnewisser M, Demaison J.

1993. *J. Mol. Spectr.* 159:62-68
56. Chapovsky PL, Papoušek D, Demaison J. 1993. *Chem. Phys. Lett.* 209:305-308
57. Jetter H, Pearson EF, Norris CL, McGurk JC, Flygare WH. 1973. *J. Chem. Phys.* 59:1796-1804
58. Nagels B, Calas N, Roozmond DA, Hermans LJF, Chapovsky PL. *Phys. Rev. Lett.* 1996. 77:4732-4735
59. Nagels B, Bakker P, Hermans LJF, Chapovsky PL. 1998. *Phys. Rev. A* 57:4322-4326
60. Gus'kov KI. 1996. unpublished.
61. Nagels B, Schuurman M, Hermans LJF, Chapovsky PL. 1995. *Chem. Phys. Lett.* 242:48-53
62. van der Meer GJ, Smeets J, Pod'yachev SP, Hermans LJF. 1992. *Phys. Rev. A* 45:1303-1306; Chapovsky PL, van der Meer GJ, Smeets J, Hermans LJF. 1992. *Phys. Rev. A* 45:8011-8018; Nagels B, Chapovsky PL, Hermans LJF, van der Meer GJ, Shalagin AM. 1996. *Phys. Rev. A* 53:4305-4310;
63. Mironenko VR, Shalagin AM. 1981. *Izvestiya Akademii Nauk SSSR, Seriya Fiz.* 45:995-1006 [Bull. Acad. Sci. USSR, Phys. Ser. 45:87]
64. van der Meer GJ, Hoogeveen RWM, Hermans LJF, Chapovsky PL. 1989. *Phys. Rev. A* 39:5237-5242
65. Chapovsky PL. 1989. *Izvestiya Akademii Nauk SSSR, Seriya Fiz.* 53:1069-1075 [Bull. Acad. Sci. USSR, Phys. Ser. 53:43-49]
66. Rautian SG, Shalagin AM. 1991. *Kinetic Problems of Nonlinear Spectroscopy*, Elsevier Sci. Publ., Amsterdam. 439 pp.
67. Hermans LJF. 1992. *Int. Rev. Phys. Chem.* 11:289-315
68. Freund SM, Duxbury G, Romheld M, Tiedje JT, Oka T. 1974. *J. Mol. Spectr.* 52:38-57
69. Nagels B. 1998. *New Light on Nuclear Spin Conversion in Molecules*, Ph.D.Thesis, Leiden University, 107 pp.
70. Nagels B, Hermans LJF, Chapovsky PL. 1997. *Phys. Rev. Lett.* 79:3097-3100
71. Chapovsky PL. 1997. The 11th International Vavilov Conference on Nonlinear Optics, June 24-27, Novosibirsk, Russia (unpublished).
72. Misra B, Sudarshan ECG. 1977. *J. Math. Phys.* 18:756-783
73. Ilisca E. 1970. *Phys. Rev. Lett.* 24:797-801
74. Ilisca E, Sugano E. 1986. *Phys. Rev. Lett.* 57:2790-94
75. Ilisca E. 1991. *Phys. Rev. Lett.* 66:667-71
76. Wigner E. 1933. *Z. f. Physik* 81:28-32
77. Oka T. 1973. *Adv. Atom. Mol. Phys.* 9:127
78. Chesnokov EN, Panfilov VN. 1977. *Zh. Eksp. Teor. Fiz.* 73:2122-2130 [Sov. Phys. JETP. 46:1112-1116]
79. Harradine D, Foy B, Laux L, Dubs M, Steinfeld JI. 1984. *J. Chem. Phys.* 81:4267-
80. Everett HO, De Lucia FC. 1989. *J. Chem. Phys.* 90:3520-3527
81. Matsuo Y, Lee SK, Schwendeman RH. 1989. *J. Chem. Phys.* 91:3948-3965

82. Shin U, Schwendeman RH. 1991. J. Chem. Phys. 94:7560-7561

83. Nagels B, Bakker P, Hermans LJF, Chapovsky PL. 1998. Chem. Phys. Lett. 294:387-390

TABLE 1. Close ortho-para level pairs in CH<sub>3</sub>F and calculated conversion rates ( $\gamma$ ) induced by spin-spin ( $SS$ ) and spin rotation ( $SR$ ) interactions.

	level pair	$\omega_{\alpha'\alpha}/2\pi^{(1)}$	$\gamma_{SS}/P$	$\gamma_{SR}/P$
Molecule	$J', K'-J, K$	(MHz)	( $10^{-3} \text{ s}^{-1}/\text{torr}$ )	( $10^{-3} \text{ s}^{-1}/\text{torr}$ )
<sup>13</sup> CH <sub>3</sub> F	11,1-9,3	130.99±0.15	7.7	–
	21,1-20,3	-351.01±0.16	4.4	1.7 <sup>(2)</sup>
<sup>12</sup> CH <sub>3</sub> F	9,2-10,0	8591.7±0.3	$9.3 \cdot 10^{-3}$	$1.3 \cdot 10^{-3}$
	15,7-17,6	1745.7±2.3	$6.8 \cdot 10^{-3}$	–
	28,5-27,6	1189.2±1.5	$16 \cdot 10^{-3}$	$\simeq 0.3^{(3)}$
	51,4-50,6	-41.3±2.5	$28 \cdot 10^{-3}$	0.1

<sup>(1)</sup>Molecular parameters for <sup>13</sup>CH<sub>3</sub>F from [34] and for <sup>12</sup>CH<sub>3</sub>F from [54].

<sup>(2)</sup>Calculated assuming spin-rotational tensor component C<sub>22</sub>=1 kHz [46].

<sup>(3)</sup>Calculated assuming spin-rotational tensor component C<sub>21</sub>=3.6 kHz and a value for  $\Gamma = 2 \cdot 10^7 \text{ s}^{-1}/\text{torr}$  [50].



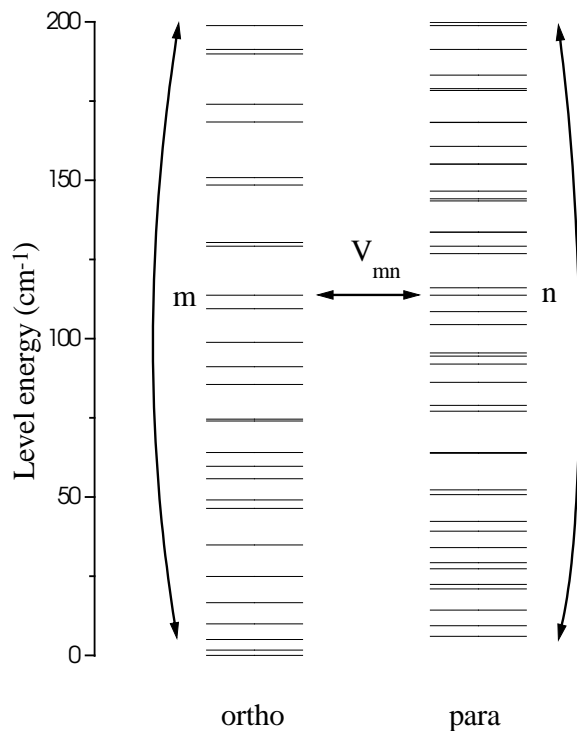


Figure 1: The rotational states of  $^{13}\text{CH}_3\text{F}$  below  $200\text{ cm}^{-1}$  in the ground vibrational state calculated using the molecular parameters from [34]. The level pair  $(J'=11, K'=1)-(J=9, K=3)$  is shown to be mixed by intramolecular perturbation  $\hat{V}$ . The bent lines indicate collisional transitions inside the ortho and para subspaces.

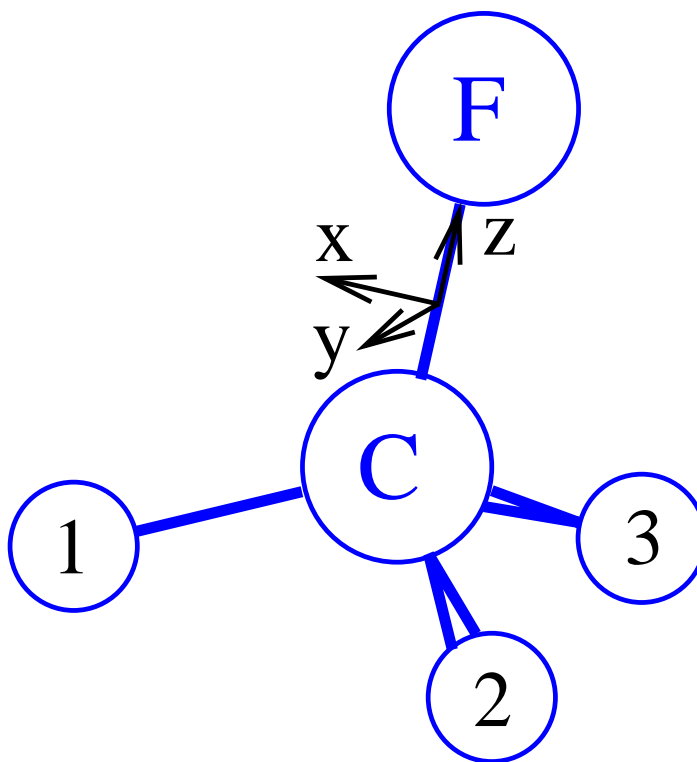


Figure 2: Numbering of the hydrogen nuclei in  $\text{CH}_3\text{F}$  and definition of the molecular coordinate system.

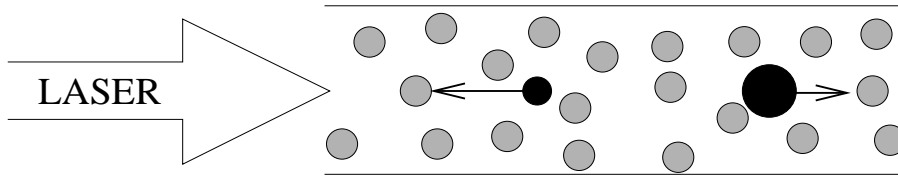


Figure 3: The principle of Light-Induced Drift (LID) [29]. Due to velocity-selective excitation combined with a state-dependent kinetic cross section, the light-absorbing species (black circles) exhibits anisotropic diffusion through the optically inert species (gray circles). Here we have assumed laser detuning in the blue wing ( $\Omega > 0$ ) and increased transport collision rate upon excitation, resulting in Light-Induced Drift of the absorbing species towards the laser.

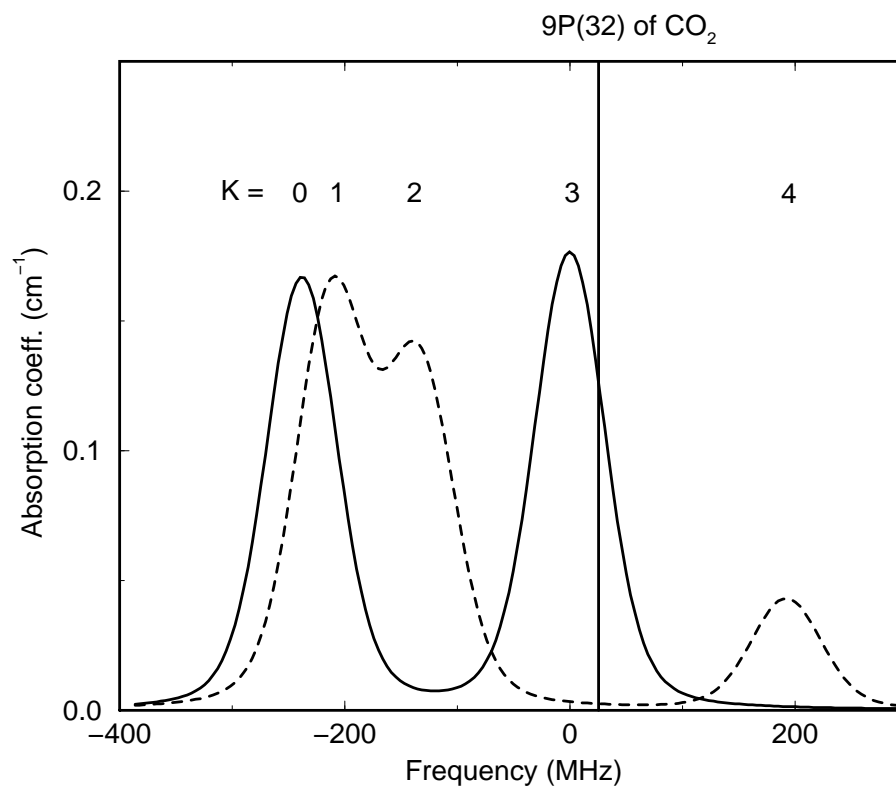


Figure 4: The  $R(4, K)$  absorption lines of ortho (-) and para (- -)  $^{13}\text{CH}_3\text{F}$  in the vicinity of the P(32) line of a CO<sub>2</sub> laser in the 9.6  $\mu\text{m}$  band. The spectrum was calculated for pressure  $P=0.5$  torr of  $^{13}\text{CH}_3\text{F}$  using the molecular parameters from [34, 68].

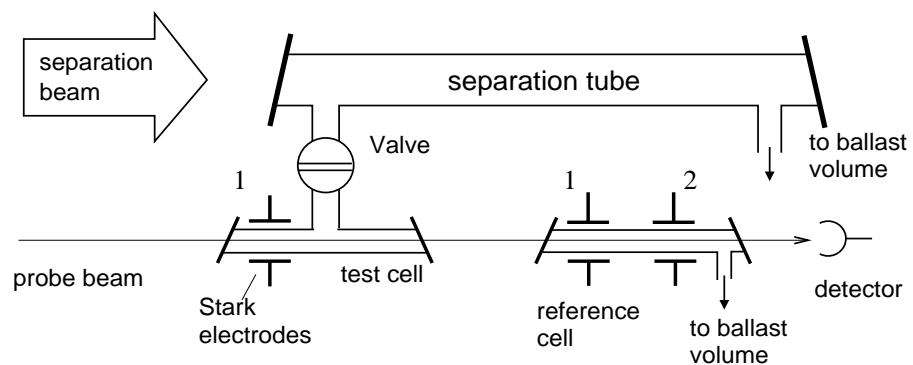


Figure 5: Schematic of the Novosibirsk setup [33]. Separation is achieved in the long upper tube. For increased sensitivity and long-term stability in detection, this differential method makes use of two detection cells with phase-shifted Stark modulation by electrodes 1 and an additional Stark modulation by electrodes 2 (see text).

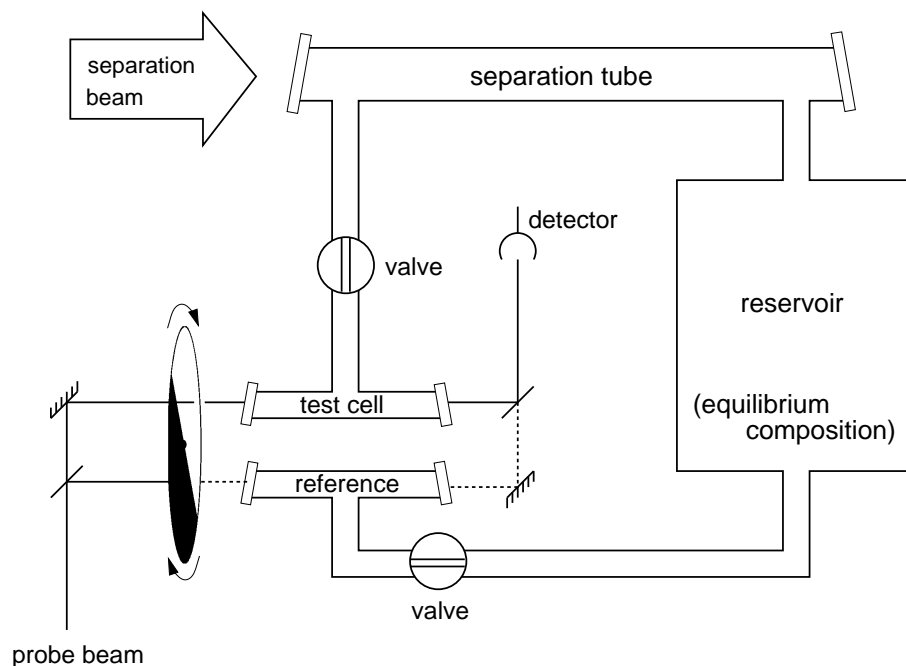


Figure 6: Schematic of the Leiden setup [41]. After separation by LID, an enriched and a reference sample are isolated by closing two valves, and the conversion process is probed by absorption. For conversion measurements at elevated temperatures a two-compartment oven was connected to the test and reference cells [59]. For conversion measurements in an electric field a Stark cell was added to the test cell [58].

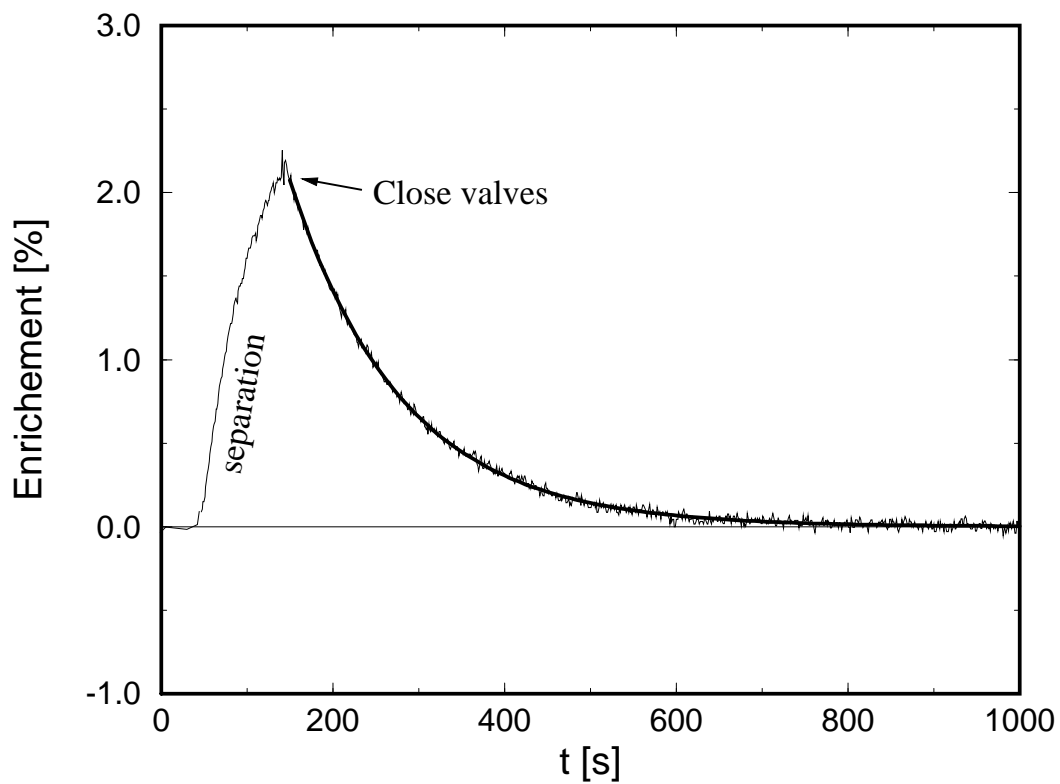


Figure 7: Typical enrichment decay curve as measured by absorption, for the  $^{13}\text{CH}_3\text{F}$  spin conversion at pressure 0.6 torr. The smooth curve is an exponential fit to the data [41].

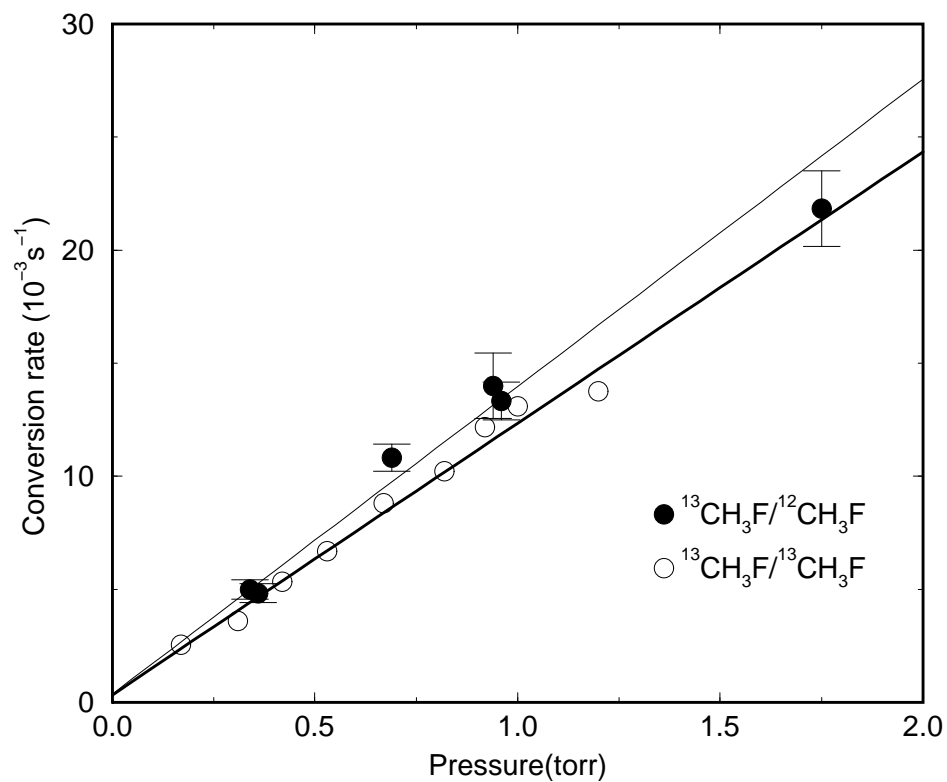


Figure 8: The pressure dependence of the  $^{13}\text{CH}_3\text{F}$  conversion rate as a function of pressure. (●) –  $^{13}\text{CH}_3\text{F}$  in  $^{12}\text{CH}_3\text{F}$  as a buffer gas [33]; (○) – pure  $^{13}\text{CH}_3\text{F}$  [41]. The solid lines give a linear fit for the two data sets.



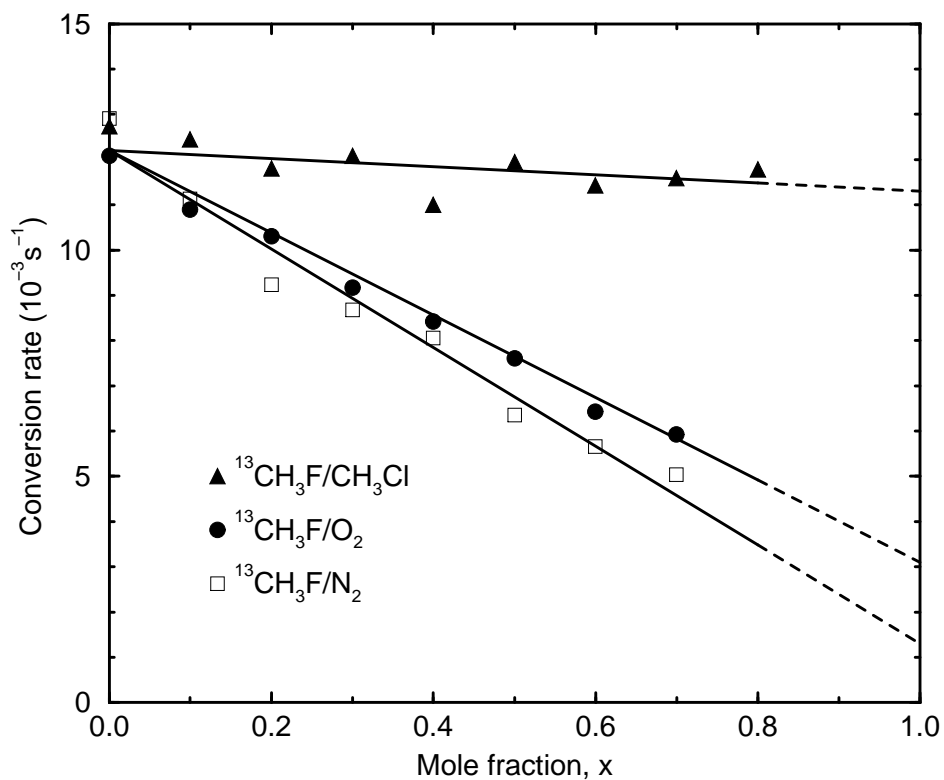


Figure 9: The  $^{13}\text{CH}_3\text{F}$  conversion rate in binary mixtures as a function of mole fraction of  $\text{CH}_3\text{Cl}$ ,  $\text{O}_2$ , or  $\text{N}_2$ . The total pressure  $P=1$  torr,  $T = 297$  K. Extrapolation to  $x = 1$  yields the conversion rate in collisions with the corresponding buffer gas [41].

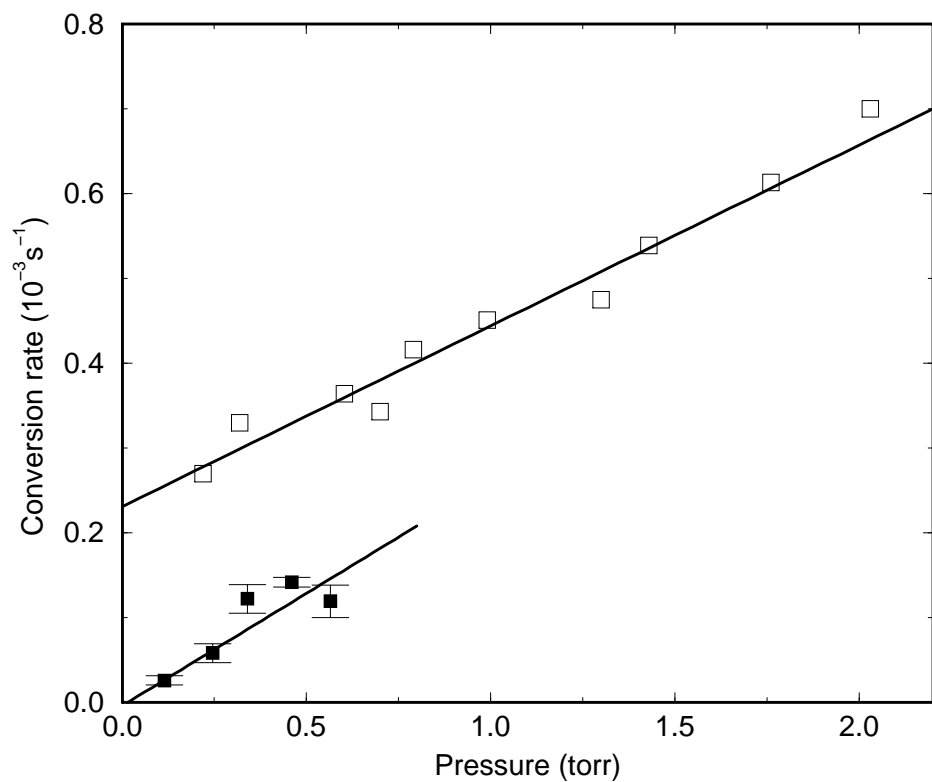


Figure 10: The pressure dependence of the conversion rate in  $^{12}\text{CH}_3\text{F}$ . Data marked by open squares are from [59]; filled squares are from [33].

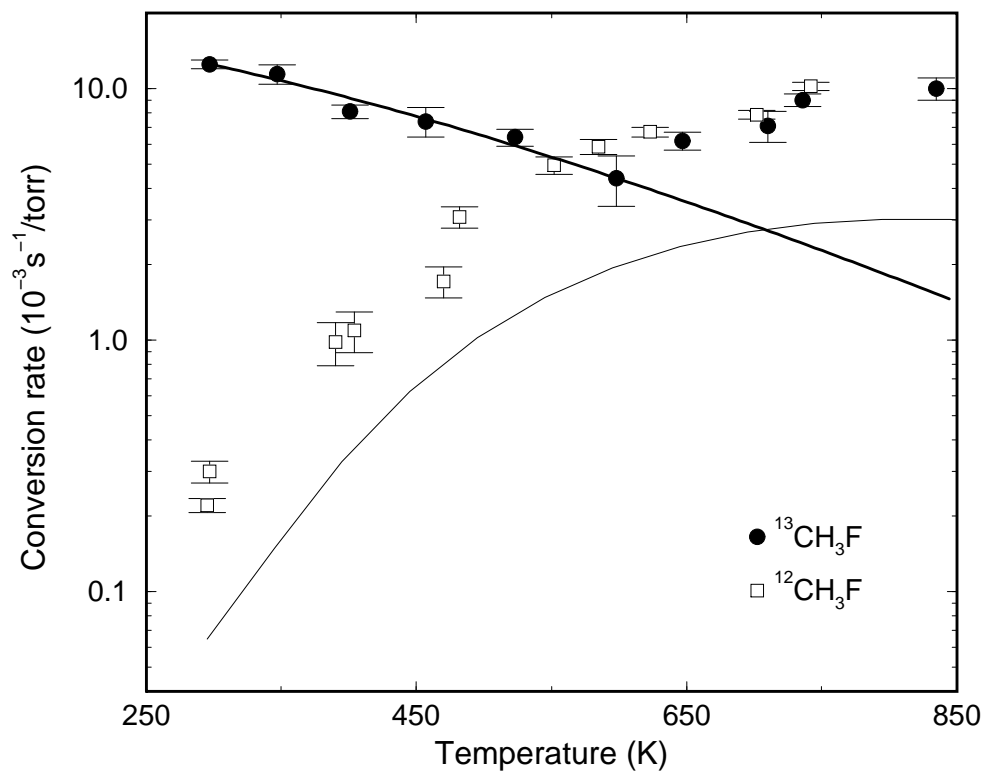


Figure 11: The conversion rates in  $\text{CH}_3\text{F}$  at various temperatures [59] (revised). The solid lines represent the calculated conversion rates in  $^{13}\text{CH}_3\text{F}$  and  $^{12}\text{CH}_3\text{F}$  assuming the same  $\Gamma(T)$  for both molecules (see Eq. (24)) and mixing of ortho and para states only by spin-spin interaction.

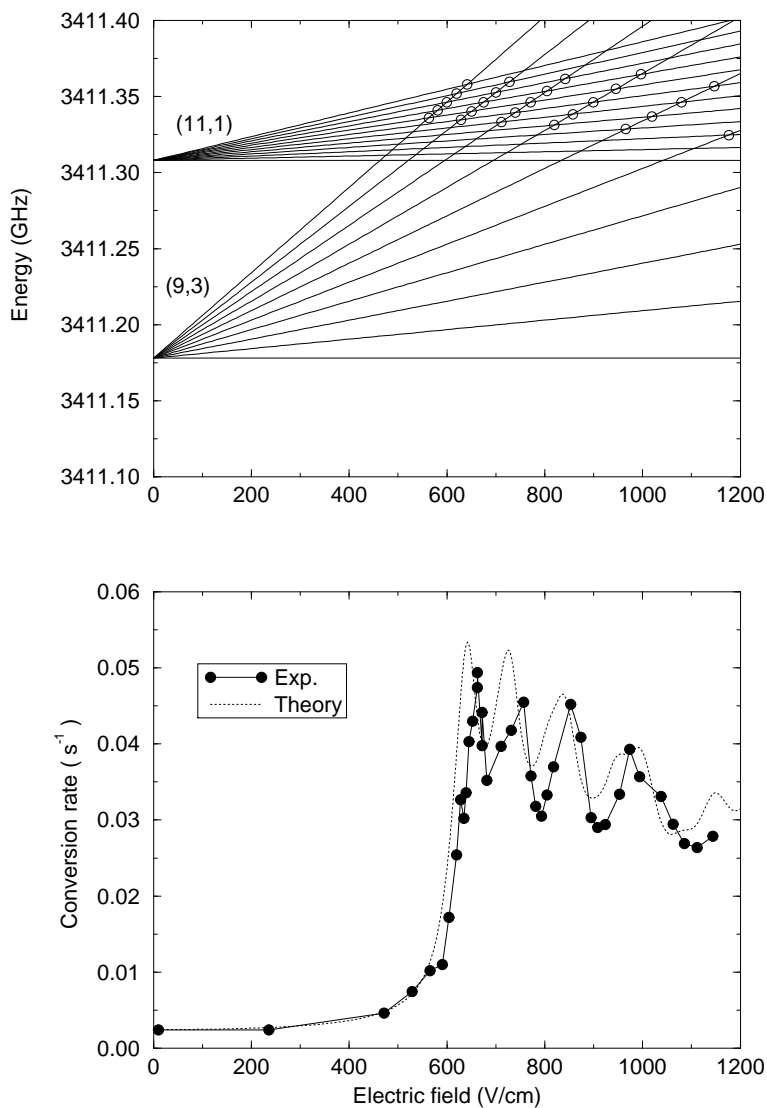


Figure 12: Upper panel: Splitting of the (11,1) and (9,3) levels by an electric field. Crossings which should contribute to the conversion through mixing by spin-spin interaction ( $|\Delta M| \leq 2$ ) are marked. Lower panel: Experimental and theoretical spin conversion rates  $\gamma(\mathcal{E})$  in  $^{13}\text{CH}_3\text{F}$  as a function of the electric field strength. Gas pressure is 0.20 torr (26.6 Pa). The experimental points are connected to guide the eye [58].

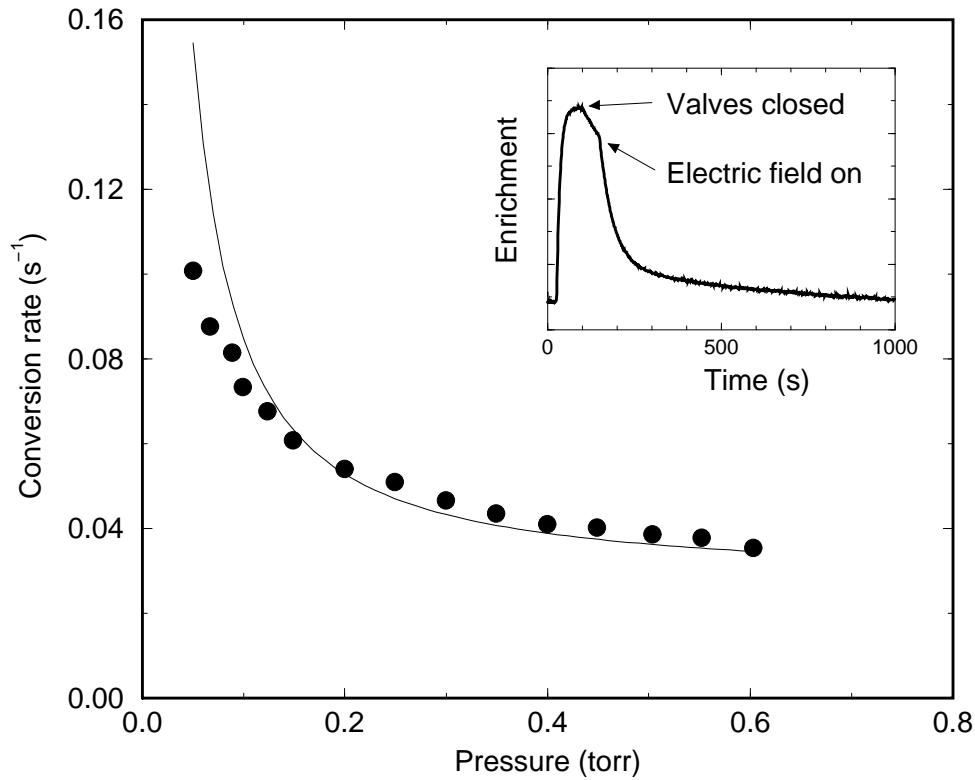


Figure 13: The ortho-para conversion rate in  $^{13}\text{CH}_3\text{F}$  as a function of pressure in a static electric field of 652.8 V/cm : experiment ( $\bullet$ ) and theory ( $-$ ). The field is chosen such that the  $M'=11$  and  $M=9$  magnetic sublevels of the levels ( $J'=11$ ,  $K'=1$ ) and ( $J=9$ ,  $K=3$ ) become degenerate (see Figure 12). The inset shows a typical decay curve [70].

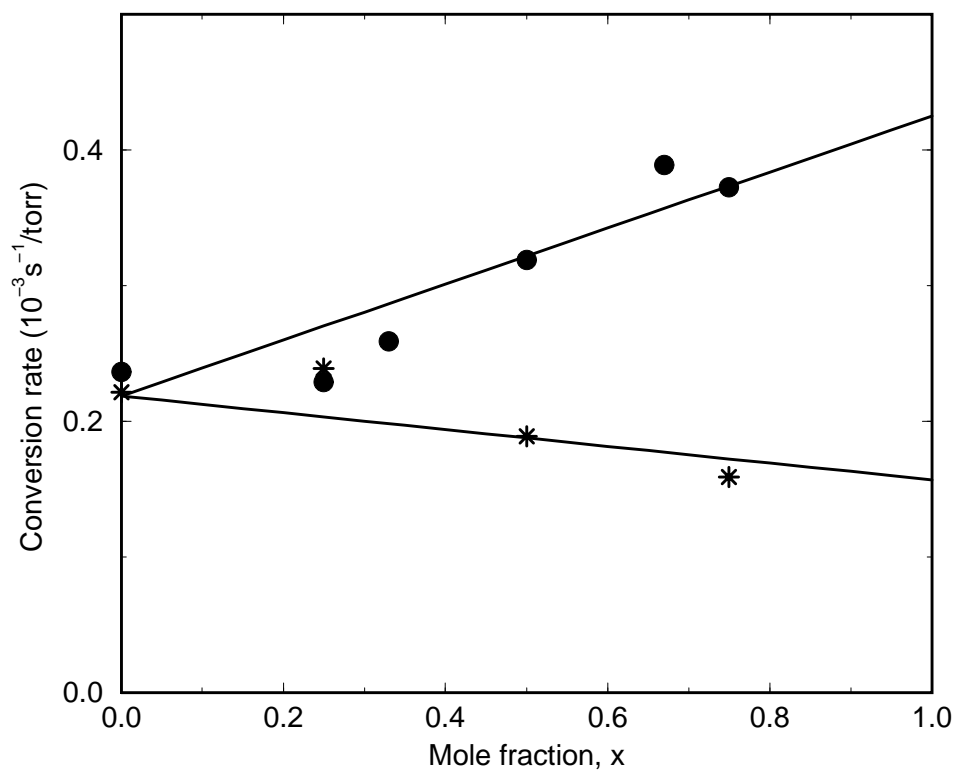


Figure 14: The experimental data for the nuclear spin conversion in  $^{12}\text{CH}_3\text{F}$  molecules as a function of mole fraction of nitrogen (\*), and oxygen (•) [83]. The total pressure is 1 torr. Note that the conversion rate increases with increasing  $\text{O}_2$  mole fraction, in contrast to the behavior of  $^{13}\text{CH}_3\text{F}$  displayed in Figure 9.